https://doi.org/10.5194/hess-2019-358
Preprint. Discussion started: 14 October 2019

Time-varying copula and design life level-based nonstationary risk analysis of extreme rainfall events

Authors: Pengcheng Xu[1], Dong Wang[*2], Vijay P. Singh[3], Yuankun Wang[2], Jichun Wu[2], Huayu Lu[1], Lachun Wang[1], Jiufu Liu[4], Jianyun Zhang[4]

[1]School of Geographic and Oceanographic Science, Nanjing University, Nanjing, P.R China

[2]Key Laboratory of Surficial Geochemistry, Ministry of Education, Department of Hydrosciences, School of Earth Sciences and Engineering, State Key Laboratory of Pollution Control and Resource Reuse, Nanjing University, Nanjing, P.R. China

[3]Department of Biological and Agricultural Engineering, Zachry Department of Civil Engineering, Texas A & M University, College Station, TX77843, USA; and National Water Center, UAE University, Al Ain, UAE

[4]Nanjing Hydraulic Research Institute, Nanjing, P.R. China

(*Corresponding author: Dong Wang, wangdong@nju.edu.cn;
Huayu Lu; huayulu@nju.edu.cn)

https://doi.org/10.5194/hess-2019-358
Preprint. Discussion started: 14 October 2019

Key points:

- The time-varying GEV model and copula models are developed for marginal and multivariate frequency analysis, respectively.
- A design life level-based risk analysis is implemented for hydraulic engineering practice.
- A systematic risk analysis incorporating nonstationarity is emphasized in comparison with stationary models.

https://doi.org/10.5194/hess-2019-358
Preprint. Discussion started: 14 October 2019

Hydrology and Earth System Sciences
Open Access
Discussions

Abstract: Due to global climate change and urbanization, more attention has been paid to decipher the nonstationary multivariate risk analysis from the perspective of probability distribution establishment. Because of the climate change, the exceedance probability belonging to a certain extreme rainfall event would not be time invariant any more, which impedes the widely-used return period method for the usual hydrological and hydraulic engineering practice, hence calling for a time dependent method. In this study, a multivariate nonstationary risk analysis of annual extreme rainfall events, extracted from daily precipitation data observed at six meteorological stations in Haihe River basin, China, was done in three phases: (1) Several statistical tests, such as Ljung-Box test, and univariate and multivariate Mann-Kendall and Pettist tests were applied to both the marginal distributions and the dependence structures to decipher different forms of nonstationarity; (2) Time-dependent Archimedean and elliptical copulas combined with the Generalized Extreme Value (GEV) distribution were adopted to model the distribution structure from marginal and dependence angles; (3) A design life level-based (DLL-based) risk analysis associated with Kendall's joint return period (JRP_{ken})and AND's joint return period (JRP_{and}) methods was done to compare stationary and nonstationary models. Results showed DLL-based risk analysis through the JRP_{ken} method exhibited more sensitivity to the nonstationarity of marginal and bivariate distribution models than that through the JRP_{and} method.

Key words: multivariate risk analysis; time-varying copula; design life level; nonstationarity; Kendall's joint return period

https://doi.org/10.5194/hess-2019-358
Preprint. Discussion started: 14 October 2019

1. Introduction

Due to climate change and increasing urbanization, heavy rains-induced floods have occurred more frequently all over the world in recent decades, which is becoming a major deterrent to the sustainable development of social economy (Mishra and Singh, 2009; Donat et al., 2016; Ali and Mishra, 2018). Various kinds of social activities, such as infrastructure constructions, agricultural irrigation and ecological maintenance would be influenced by hydrometeorological extreme events. A systematic risk analysis of these extreme events would provide sufficient strategies for decision makers.

A multitude of studies have addressed the effect of climate change and urbanization on hydrological design to alleviate associated risks. Traditional hydrological frequency analysis or risk analysis is based on the stationary assumption, which recommends that environmental impact indexes, such as climatic factors and land use rate, have a constant mechanism or pattern that affects hydrological variables all the time (Madsen et al., 2017; Milly et al., 2015). The feasibility of hydrological frequency and risk analysis based on stationary assumptions is being challenged because of the multiple effects of climate change, urbanization, and heat island effects. Accordingly, water authorities should amend the present planning, design and management strategies to develop nonstationary distribution models based on the signals of climate change. Therefore, it is urgent to develop an efficient and systematic risk analysis approach from time dependent side to serve for hydraulic design of hydrological infrastructures to cope with the effect of climate change.

https://doi.org/10.5194/hess-2019-358
Preprint. Discussion started: 14 October 2019

In recent years, nonstationary hydrological frequency analysis has received a great deal of attention because of increasing attention to climate change (Chen and Sun, 2017; Call et al., 2017; Ghanbari et al. 2019). The time-varying moment approach is widely used to involve time variant probabilistic parameters for mimicking the changing behavior of extreme hydrometeorological variables. Nonstationarity modeling of probability distribution has been conducted for univariate cases in recent years (Zhang et al., 2015; Ganguli and Coulibaly, 2017; Agilan and Umamahesh, 2018).

Du et al. (2015) modelled nonstationary low-flow series in Weihe River basin, China, based on the Generalized Additive Models in Location, Scale and Shape (GAMLSS) framework. Results showed that inappropriately estimated statistical parameters would lead to the overstatement of risk corresponding to a low-flow event. Gu et al. (2016) incorporated time, climate indices, precipitation, and temperature into the GAMLSS model to detect nonstationarity in flood frequency. For the univariate case, nonstationary risk analysis, based on the time-varying moment approach, can be decomposed into four steps: (1) Descriptive and exploratory monitoring of hydrological sequences and monitoring of outliers; (2) implementation of the stationarity hypothesis to verify the nonstationarity of hydrological series; (3) development of a hydrological frequency analysis model and estimation of model parameters using different covariates; and (4) risk assessment based on the selected frequency model.

The above studies were conducted under nonstationary conditions for univariate cases, while it is known that natural hydrometeorological extreme events are

https://doi.org/10.5194/hess-2019-358
Preprint. Discussion started: 14 October 2019

multivariate, characterized by multi-attribute properties which can be statistically correlated. For instance, floods are characterized by volume, peak, and duration, while extreme rainfall events have the attributes of duration, intensity, total amount. As a result, univariate nonstationary risk analysis cannot fully encompass the dependence structure between hydrological attributes. It is therefore desirable to develop a multivariate model to simulate the probabilistic behavior of two or more properties. Copulas, a useful tool for modelling the structure of dependence between hydrological variables regardless of the types of marginal distributions, have been widely used for multivariate frequency analysis of rainfall extreme events (Zhang and Singh, 2007; Kao and Govindaraju, 2008; Rauf and Zeephongsekul, 2014; Vandenberghe et al., 2010); droughts (De Michele et al., 2013; Serinaldi et al., 2009; Shiau, 2006; Song and Singh, 2010; Wong et al., 2010); floods (Grimaldi and Serinaldi, 2006; Zhang and Singh, 2006). However, these studies assumed a time invariant dependence pattern, ignoring the influence of climate change and hence did not consider the impact of nonstationarity on the dependence structure.

Recently, studies on multivariate distribution fitting have addressed the superiority of dynamic copula-based method to model the nonstationary dependence structure, which are generally caused by complex environment and rapid urbanization (Milly et al., 2015). Former studies have detected nonstationarity in dependence structures (Liu et al. 2017; Assia et al., 2014; Yilmaz and Perera, 2014). Chebana et al. (2013) argued that it was necessary to determine a multivariate distribution model quantifying the time-varying dependence structure of various kinds of hydrological variables. Bender et al. (2014) used a bivariate nonstationary multivariate model with a 50-year moving time window to investigate the time-dependent behavior in bivariate case. Their results showed that the joint probability varied significantly over time for different non-stationary models. Jiang et al. (2015) also did a multivariate risk analysis using the time-varying copula method incorporating time and reservoir index as covariates for low-flow series extracted from two neighboring observed stations.

Traditional solutions of hydrological extreme events involve return period-based methods, which are usually calculated as the inverse of annual exceedance probability for a given magnitude under stationary conditions in a univariate case. In a multivariate case, the univariate return period can be extended to joint return periods of hydrological variables. There are three kinds of joint return period methods to quantify the exceedance probability of a multivariate extreme event: the OR method that at least one extreme attribute is larger than the specified threshold; the AND method that all the attributes are larger than the specified threshold; and the Kendall method that the univariate value derived from the Kendall distribution function according to a specified value (Jiang et al., 2015; Salvadori and Michele, 2010; Salvadori et al., 2013). While non-stationary distribution models provide flexibility to analyze the variability of a hydrological variable, they are also incongruent with many of the traditional metrics used in water resources planning. For example, the development of drainage standards are vulnerable to the standard of extreme rainfall return period, which means drainage facilities have been designed to withstand the extreme rainfall event of a specified return period. The multivariate hydrologic and hydraulic design can be influenced by the existence of nonstationarity in both the marginal and joint distributions. The exceedance probability of a given extreme event would be different from year to year, leading to a nonconstant and non-unique value of the conventional return period. Thus, the notion of static return period of an extreme rainfall event (e.g., 100-year extreme rainfall event, 200-year extreme rainfall event) is no longer reliable for hydraulic design under nonstationary conditions (Salas and Obeysekera, 2014; Yan et al., 2017). As a result, Rootzén and Katz (2013) first mentioned the concept of design life level (DLL) to quantify the risk of a given extreme rainfall magnitude over the hydrological structure's life time (Note that following the idea of Rootzén and Katz (2013) we regard the term hydrological risk as the possibility of a certain extreme event occurring and not as a quantification of expected losses). It is a logical extension to handle the nonstationarity of the concept of "risk of failure" (Jakob, 2013), which is more frequently used to quantify the risk of hydrologic extremes under stationarity. Read and Vogel (2015) extended the DLL method to average annual reliability (AAR) method to estimate the hydrologic design value considering nonstationarity. In general, these risk-based methods can provide similar results of hydraulic design for hydrological infrastucture (Yan et al., 2017). However, the cases of multivariate hydrologic designs, especially under nonstationary conditions using the time-varying copula, and design life level-based risk methods have great potentiality in future studies.

https://doi.org/10.5194/hess-2019-358
Preprint. Discussion started: 14 October 2019

Therefore, the objective of this study is to do risk analysis of multivariate extreme rainfall events involving the following steps. First, a series of statistical tests, such as Ljung-Box test, and univariate and multivariate Mann-Kendall and Pettist tests are used for both the marginal distributions and the dependence structures to determine different forms of nonstationarity (sudden jump, periodicity, and trend). Second, a nonstationary multivariate probability distribution is developed using a time-varying GEV and copula-based model, which can encompass the nonstationarities probably existed in marginal and joint distributions. Finally, design life level-based risk analysis is extended to multivariate cases through Kendall's joint return period and AND's joint return period methods. In this paper, we investigated two kinds of extreme rainfall attributes: (1) annual extreme rainfall volume (*Ps*: Annual total precipitation of the daily precipitation more than the 95th percentile threshold) and intensity (*Im*: Annual maximum daily precipitation), through the nonstationary multivariate risk analysis method. The remainder of this paper is organized as follows. The next section presents the methodology adopted in this study. Section 3 discusses the results of proposed model applied to Haihe River basin, China. Section 4 presents the final conclusion through the proposed model.

2. Methodology

Copulas are tools to build multivariate distribution models of dependence structures between random variables regardless of their marginal distribution types. Detailed information about copulas can be found in Nelson (2007). The present copula-

https://doi.org/10.5194/hess-2019-358
Preprint. Discussion started: 14 October 2019

based methods to solve the multivariate risk analysis mostly adopt static parameters for whether the marginal distribution or joint distribution. The changing climate has led to nonstationarity of individual hydrological series or the dependence between hydrological variables. To realize this situation, a time-varying copula-based model can describe the time dependent characteristics for dependence structure of hydrological variables, as inspired by Patton (2006) from the financial field.

Let (x, y) represent a hydrological pair. The joint probability distribution of multivariables through time-varying copula model can then be presented as:

$$F_{X,Y}(x,y) = C[F_X(x|\theta_X^t), F_Y(\mathrm{y}|\theta_Y^t)|\theta_C^t] = C(u,v|\theta_C^t) \quad (1)$$

where $C(\cdot)$ denotes the copula function; $F_{X,Y}(\cdot)$ denotes the joint function; $F_X(\cdot)$ and $F_Y(\cdot)$ represent the marginal functions of hydrological variable (*Ps* and *Im* in this study); θ_X^t and θ_Y^t represent the time-varying marginal distribution parameters; θ_C^t is the dynamic copula parameter which is a linear function of time; and u and v are the marginal probabilities in the time-varying copula in the hypercube unit.

In the framework of multivariate risk analysis (**Figure 1**), the property of nonstationarity can be determined not only by one or two marginal variables but also in the dependence structure or vice versa. It is however possible that the nonstationary behavior may exist in both the marginal and joint distribution function. To determine the nonstationarity (mutation, cyclicity and trend) in the synthetized extreme rainfall attribute series, statistical tests, such as Ljung-Box test, and univariate and multivariate Mann-Kendall and Pettist tests are used for both the marginals and the dependence

https://doi.org/10.5194/hess-2019-358
Preprint. Discussion started: 14 October 2019

structure. Details of these tests can be found in the references due to (Serinaldi and Kilsby, 2016; Chebana et al., 2013; Rizzo and Székely, 2010).

As shown in **Figure 1**, the time-varying copula-based risk analysis model can be decomposed into three main phases: (1) detection of nonstationarity in the marginal variables and dependence structure through a series of nonparametric tests; (2) estimation of the time-varying parameter for the marginal and joint probabilty distributions; and (3) joint return period and risk analysis by design life level-based risk methodology from the perspectives of Kendall's and AND's return period methods (detailed information can be found in Section 2.3).

Insert **Figure 1** here.

2.1. Time-varying marginal distribution

In this part, the Generalized Extreme Value (GEV) distribution was used to establish time-varying marginal distribution model for the extreme rainfall attributes because it is a good aggregation of the Gumbel, Fréchet, and Weibull distributions and is especially suitable for extreme data sets (Cheng and AghaKouchak, 2014). Let $F(x)$ be the cumulative probability distribution function (CDF) of the quantity of interest, *Ps* or *Im*, in this study. The GEV distribution consists of three control parameters, the location, the scale, and the shape, which describe mean value of the sample series, amplitude near the location, and the tail of the distribution, respectively. The cumulative

https://doi.org/10.5194/hess-2019-358
Preprint. Discussion started: 14 October 2019

distribution of GEV model under stationary conditions can be expressed as follows:

$$F(x) = \begin{cases} \exp\left\{-\left[1+\kappa\left(\frac{x-\mu}{\sigma}\right)\right]_+^{-\frac{1}{\kappa}}\right\} & \text{if } \kappa \neq 0 \\ \exp\left\{-exp\left(-\frac{x-\mu}{\sigma}\right)_+\right\} & \text{if } \kappa \to 0 \end{cases} \quad (2)$$

where z_+=max{y,0} and

$x \epsilon [(\mu-\sigma)/\kappa, +\infty)$ when $\kappa > 0$,

$x \epsilon (-\infty, (\mu-\sigma)/\kappa]$ when $\kappa < 0$, and

$x \epsilon (-\infty, +\infty)$ when $\kappa = 0$.

where μ denotes the location parameter, σ is the scale parameter and κ is the shape parameter. In this study, two kinds of nonstationary GEV models (GEVns-1 and GEVns-2) are developed with the shape parameter being constant. It should be emphasized that modelling the time variance in shape parameter needs long-term observations, which are often not available in practice (Cheng et al., 2014). GEVns-1 model considers the time-varying characteristic of the location parameter only, while GEVns-2 model incorporates the time varying features of both location and scale parameter. These two nonstationary models regard significant trends as a linear function of time (in years):

$$\mu(t) = \mu_o + \mu_1 t \quad (3)$$

$$\sigma(t) = \exp(\sigma_o + \sigma_1 t) \quad (4)$$

where the scale parameter is always positive throughout, it is usually calculated on the basis of a log link function.

In this study, the Bayesian method through the Markov chain Monte Carlo

https://doi.org/10.5194/hess-2019-358
Preprint. Discussion started: 14 October 2019

(MCMC) approach (Cheng et al., 2014) was used to estimate the nonstationary GEV model. Simultaneously, the Deviance Information Criterion (*DIC*) and Bayes factors (*BF*) for different stationary and nonstationary models were calculated to select the best fitted marginal model. The minimum *DIC* value yielded the best performance, while BF smaller than 1 indicated the best fitting.

2.2. Time-varying Copula

To model the dependence structure between annual total precipitation (*Ps*) and annual daily maximum precipitation (*Im*) under nonstationary conditions, a time-varying copula was developed. In multivariate hydrological frequency analysis, two kinds of copulas, named elliptical and Archimedean copulas are widely used in hydrological applications. In this study, time-varying elliptical copulas, Student t (St) copula, as well as the widely-used time-varying Archimedean copulas, time-varying Clayton, Gumbel and Frank copula, were selected as candidate models to simulate the time-varying dependence between two extreme rainfall attributes. The Gaussian copula was not used in this study because of its deficiency in describing dependencies of extremes (Renard and Lang, 2007).

The copula parameter θ_C^t can be assumed as a linear function of the time ("year" in this study) and can be defined as follows:

$$\theta_C^t = \begin{cases} \exp(\beta_o + \beta_1 t) & \theta_c > 0 \\ \beta_o + \beta_1 t & \theta_c \in R \end{cases} \tag{5}$$

where $\theta_c > 0$ denotes the Student t (St), Clayton and Gumbel copula, while $\theta_c \in R$ represents the Frank copula.

https://doi.org/10.5194/hess-2019-358
Preprint. Discussion started: 14 October 2019

The maximum pseudo-likelihood (MPL) method was adopted to estimate the time-varying copula parameter (Genest et al., 1995). The Corrected Akaike Information Criterion (AICc; Hurvich and Tsai, 1989) was employed to make a goodness-of-fit, which is a modified version of AIC for small samples. Obviously, the presence of nonstationarity in the copula parameter was determined by comparison of the AICc value.

2.3. Joint return period and risk analysis based on KEN's and AND's methods

For hydrological management, engineering administrators focus more on the return period and risk of failure during the design life of hydraulic structures (Condon et al., 2015). Inspired by design life level (DLL) method to present the risk proposed by Rootzén and Katzs (2013), we would like to expand the DLL-based risk to the multivariate case.

Let *F(X)* be the cumulative probability distribution function (CDF) of the quantity of interest, in this study, maximum daily precipitation in a year (*Im*). Conventionally, the *T*-year return level for certain daily precipitation x_T is equal to the (1-1/*T*)-th quantile of the marginal distribution of *Im* (The probability distribution is the same for all years in a stationary situation.). Equivalently, on average, one out of *T* years has at least one daily rainfall that exceeds x_T, so that $T\left(1 - F(x_T)\right) = 1$(Serinaldi and Kilsby, 2015), and the probability of annual maximum daily rainfall exceeds x_T is 1/*T*.

Then, the hydrological risk *R* (i.e. risk of failure) of a certain hydraulic structure for a design life of *n* years can be expressed as the probability that at least one rainfall

https://doi.org/10.5194/hess-2019-358
Preprint. Discussion started: 14 October 2019

extreme exceeds the design level x_T in a period of *n* years. Under stationary conditions, the probability of annual maximum daily rainfall exceeding x_T in every year is the same as 1/*T*. In a univariate context, hydrological stationary risk can be defined as (Fernandez and Salas, 1999; Serinaldi and Kilsby, 2015):

$$R_s = 1 - F(x_T)^n = 1 - (1 - 1/T)^n \tag{6}$$

Considering time-varying exceedance probabilities, the probability of annual maximum daily rainfall exceeding x_T in each year is different. So here we use $F_t(x_T)$ to represent the probability of daily rainfall exceeding design level x_T in the *t*-th year. So the design life level-based nonstationary risk for the univariate case is:

$$R_{ns} = 1 - \prod_{t=1}^{n} F_t(x_T) \tag{7}$$

From the perspective of bivariate case, the joint return period (JRP) of extreme rainfall events can be calculated through three methods in a stationary situation (Salvadori et al., 2011). They are AND method corresponding to the probability of $P(X \geq x \cap Y \geq y)$, OR method corresponding to $P(X \geq x \cup Y \geq y)$, and Kendall return period method (KEN). Details of the Kendall return period can be found in Salvadori and De Michele (2004). Since the AND method is widely used and the Kendall method is of great potentiality, we expanded the AND method and the Kendall return period method to the nonstationary case here. Let JRP_{s-and} and JRP_{s-ken} represent the three types of return period in the stationary case; they can be calculated as follows:

$$JRP_{s-and} = \frac{1}{P((X \geq x \cap Y \geq y))} = \frac{1}{1 - F_X(x) - F_Y(y) + C[F_X(x), F_Y(y)]} \tag{8}$$

$$JRP_{s-ken} = \frac{1}{P\{C[F_X(x), F_Y(y)] \geq p_{ken}\}} = \frac{1}{1 - K_c(p_{ken})} \tag{9}$$

where $K_c(\cdot)$ is the Kendall distribution function which can be defined as:

$$K_c(p_{ken}) = P\{C[F_X(x), F_Y(y)] \leq p_{ken}\} \tag{10}$$

Here, $F_X(x)$ and $F_Y(y)$ are the marginal cumulative probability distribution functions (CDF) for *Ps* and *Im*, respectively, while $C[F_X(x), F_Y(y)]$ is the bivariate copula function connecting these two extreme attributes. p_{ken} is just the critical probability level corresponding to $K_c(p_{ken})$.

Similar to the JRPs of extreme rainfall events under stationary case, the JPRs of AND and KEN in nonstationary situations can be achieved by:

$$JRP_{ns-and} = \frac{1}{1 - F_X(x|\theta_X^t) - F_Y(y|\theta_Y^t) + C[F_X(x), F_Y(y)|\theta_C^t]} \tag{11}$$

$$JRP_{ns-ken} = \frac{1}{1 - K_c^t(p_{ken})} \tag{12}$$

where θ_X^t, θ_Y^t and θ_C^t represent the time variant parameters of the marginal and copula distributions; and $K_c^t(p_{ken})$ is the time-varying Kendall distribution function corresponding to the time-varying copula.

Multivariate extreme value analysis should be focused on the most likely extreme event with the largest copula density. The most likely event at the T_0-year level can be calculated as (Graler et al., 2013):

$$(u_m, v_m) = \underset{T_0}{\operatorname{argmax}}\, c(u, v) \tag{13}$$

The most likely design combinations (x_m, y_m) can be computed according to the inverse of marginal cumulative distribution function:

https://doi.org/10.5194/hess-2019-358
Preprint. Discussion started: 14 October 2019

$$x_m = F_X^{-1}(u_m) \text{ and } y_m = F_Y^{-1}(v_m) \tag{14}$$

where u, v are the marginal distribution functions of X and Y. Let two pairs of extreme rainfall attributes $(x_{m_1}, y_{m_1})_{T_0^{and}}$ and $(x_{m_2}, y_{m_2})_{T_0^{ken}}$ be the most likely design combinations of *Ps* and *Im* at the T_0-year level for JRP_{s-and} and JRP_{s-ken}. Similar to the nonstationary risk calculation in the univariate case, the hydrological nonstationary DLL-based risk in the bivariate case can be calculated from two circumstances:

$$R_{ns-and} = 1 - \prod_{t=1}^{n} \{F_X(x_{m_1}|\theta_X^t) + F_Y(y_{m_1}|\theta_Y^t) - C[F_X(x_{m_1}), F_Y(y_{m_1})|\theta_C^t]\} \tag{15}$$

$$R_{ns-ken} = 1 - \prod_{t=1}^{n} K_c^t(p_{ken})_{(x_{m_2}, y_{m_2})} \tag{16}$$

where R_{ns-and}, R_{ns-ken} indicate the nonstationary risk for a design life level of *n* years in the bivariate case corresponding to two types of joint return period. The stationary risk can be calculated in the same way with marginal and copula distribution parameters being constant.

In this study, comparison of hydrological risk for the bivariate case between stationary and nonstationary models can be quantified by the risk changing rate $\Delta R_{T_0}^n$ which can be calculated as:

$$\Delta R_{T_0}^n = \frac{1}{n} \sum_{i=1}^{n} \frac{|R_i^{ns} - R_i^s|}{R_i^s} \tag{17}$$

where R_i^{ns} and R_i^s are nonstationary risk and stationary risk of a certain hydraulic structure for a design life of *i* years. $\Delta R_{T_0}^n$ helps quantify the difference in risk between stationary and nonstationary models.

https://doi.org/10.5194/hess-2019-358
Preprint. Discussion started: 14 October 2019

3. Application

3.1. Study area and data collection

The area selected for the study is Haihe River basin, China, which belongs to the temperate East Asian monsoon climate zone (**Figure 2**). In summer, heavy rains take place and temperature and humidity are high caused by marine air masses. The annual rainfall has a great spatial and temporal variability across the basin due to the inconsistency of intensity, retreat time and influence of the Pacific subtropical high over the years. Natural disasters, such as urban floods and mountain torrents induced by extreme rainfall events in the basin have caused huge losses to the social economy and people's lives and property, and have been highly valued by decision-making authorities. As a result, time-varying copula-based multivariate risk analysis of this basin is conducive to providing reliable strategies and alternative options for water resources risk-based decision making.

Daily rainfall data from Haihe River basin observed at Wutaishan, Fengning, Zhangjiakou, Beijing, Tianjin, and Nangon were analyzed for the proposed nonstationary model. Detailed information on these six gauges is presented in Table 1. According to various data ranges shown in **Table 1**, the rainfall series from 1958-2017 was selected as the final version.

Insert **Figure 2** Here.

Insert **Table 1** Here.

https://doi.org/10.5194/hess-2019-358
Preprint. Discussion started: 14 October 2019

4.2. Preprocessing Analysis

Before developing a nonstationary frequency analysis model, it is essential to examine nonstationarities of extreme precipitation attributes (*Ps* and *Im*) as well as the structure of dependence between these two attributes. A series of statistical tests (i.e. Ljung-Box test, univariate and multivariate Man-Kendall tests, and univariate and multivariate Pettitt tests) were performed to detect the nonstationarity in extreme precipitation time series. Trends in the time series can be evaluated using various tests (Lima et al., 2016; Yilmaz et al., 2017; Sarhadi and Soulis, 2017). **Table 2** shows results of tests detecting nonstationarity, while **Figure 3** shows the spatial distribution of trends and change points for two attributes of rainfall extremes (*Ps* and *Im*) as well as the dependence structure between them. First, time series of these two rainfall extremes (*Ps* and *Im*) for all 6 stations can pass the Ljung-Box test with 20 lags (p.value>0.05 in **Table 2**). Extreme observations are mutually independent with no serial autocorrelation, so it is appropriate to apply the standardized Mann-Kendall test to evaluate the statistical significance of trend without any modification (Serinaldi and Kilsby, 2016).

As shown in **Figure 3**, concurrences of univariate and bivariate trends, the nonstationarities in rainfall extremes can be detected at several stations (stations 2, 3, and 4). Station 1 exhibits a significant nonstationarity for extreme attribute *Ps*, while extreme attribute *Im* and dependence structure show an insignificant decreasing trend. On the other hand, stations 5 and 6 show a weak decreasing trend. The above tests

https://doi.org/10.5194/hess-2019-358
Preprint. Discussion started: 14 October 2019

totally recommend the presence of nonstationarities in extreme series as well as the dependence pattern across three out of 6 sites. According to Porporato and Ridolfi (1998), an insignificant trend should not be ignored because of its effect on the results of hydrological risk analysis. Hence, even if precipitation extremes at a certain station may recommend statistically weak trends, both the nonstationary and stationary models are established for each station in the following section.

Insert **Table 2** Here.

Insert **Figure 3** Here.

4.3. Marginal distribution fitting

The nonstationarity can appear either in univariate variables or in dependence structure in the multivariate framework (Bender et al., 2014). Results of trend and change point tests performed in Section 4.1 pointed out the necessity to take the nonstationarity of marginal distributions into consideration. In this study, the Generalized Extreme Value (GEV) distribution which is a good hybrid of the Gumbel, Fréchet, and Weibull distributions fits the block or annual maximum time series better (Cheng et al., 2014). **Table 3(a)-(b)** shows performances of nonstationary vs. stationary models for these six stations. The location parameter (μ) and scale parameter (σ) are regarded as time variant, while the shape parameter κ is time invariant; it should be noted that modeling of time-varying κ requires a sufficiently long record of

https://doi.org/10.5194/hess-2019-358
Preprint. Discussion started: 14 October 2019

observations (Cheng et al., 2014). Despite the exception of *Im* for station 4, the shape parameter κ for most fitted models was in the interval of [-0.3,0.3] which is in accordance with the previous study (Martins and Stedinger, 2000; Ganguli and Coulibaly, 2017). The best fitted model was selected by performing the minimum *DIC* criterion combined with the Bayes factor (*BF*) test. For instance, the GEV_{ns}-2 model (nonstationary GEV model with time varying location and scale parameters) was the best selected model for the extreme attribute *Im* extracted from station 1. That was because the BF values of GEV_{ns}-2 and GEV_{ns}-1 were both smaller than 1 which meant that these two nonstationary models passed the BF test. Then, the best fitted nonstationary model GEV_{ns}-2 for *Im* of station 1 was achieved following the *DIC* test. Similarly, the best fitted marginal distribution of two extreme rainfall attributes for all these six stations was selected. Except for stations 4 and 5, the best distributions for the other stations were parallel for nonstationarity tests shown in Section 4.1.

Insert **Table 3(a)-(b)** here.

4.4. Copula fitting

Elliptical and Archimedean (Clayton, Gumbel, and Frank) copulas have been widely applied in hydrological practice. In this study, time-varying elliptical copulas, Student t (St) copula, as well as Clayton, Gumbel and Frank copulas were selected as alternative models to simulate the dependence structures of extreme attributes. The

https://doi.org/10.5194/hess-2019-358
Preprint. Discussion started: 14 October 2019

Gaussian copula was not used in this study because of its deficiency in describing dependencies of extremes (Renard and Lang, 2007). Once a marginal distribution was estimated based on test statistics, the dependence structure for *Im* and *Ps* was described by the time-varying or time invariant copula functions. **Table 4(a)-(b)** illustrates the results of best fitted copula, based on the minimum AICc and maximum log-likelihood value (LL). The time-varying Student t (St) copula exhibited the best performance among the eight candidate copulas (four stationary copulas as well as the corresponding nonstationary copulas) for stations 1, 2, 3, 4, and 6, while the stationary St copula was the best one for station 5 which meant that results of dependence structure modelling for station 5 did not indicate any nonstationarity signal which was reasonable, according to multivariate MK and Pettit tests of station 5 (**Table 2**). Contrary to station 5, the nonstationary St copula fitted better than did the stationary model for stations 1 and 6 which was not in accordance with the nonstationarity tests for these two stations (**Table 2**). Based on the above results, an insignificant trend or weak change point would lead to a nonstationary probability function of dependence patterns to some extent (Porporato and Ridolfi, 1998) which should be dealt with cautiously.

With the best fitted marginal distributions and the best copula, the quantiles of extreme rainfall attributes (*Ps* and *Im*) were derived from the pseudo-observations ranging from 0 to 1 in order to provide a benchmark for return period and risk analysis for hydrological and hydraulic design. The method of analysis is presented in the following section.

https://doi.org/10.5194/hess-2019-358
Preprint. Discussion started: 14 October 2019

Insert **Table 4(a)-(b)** here.

4.5. Nonstationary return period and risk analysis for univariate and bivariate cases

(1) Univariate return period: Once parameters of the best fitted models for univariate and bivariate cases have been estimated, the extreme rainfall quantiles for certain return levels (T) can be simulated. In this section, return period and risk analysis was performed by comparing stationary and nonstationary models. The estimated rainfall quantiles (*Ps* and *Im*) versus time in the univariate case are shown in Figures 4 for the six stations of Haihe River. *Im* and *Ps* for stations 4 and 6 are not provided, because the best marginal model for the extreme attributes of these two stations was the stationary GEV model (**Table 3**). In the case of *Ps* for station 1 shown in **Figure 3**, a 100-year *Ps* quantile under stationary circumstances (GEV_s model with dashed red line in **Figure 3**) (355 mm) corresponded to a 35-year *Ps* under nonstationary conditions (GEV_{ns-2}) in the year 1960 and a 60-year *Ps* in the year 1970. In other words, an exceedance probability of 0.01 increased to 0.028 and 0.017. On the other hand, the return period associated with a given quantile decreased from 1960 to 2020 for *Im* of station 4 and *Ps* of station 5, while the return period increased for extreme attributes of other stations. Interestingly, the temporal variability between different stations corresponding to the best selected nonstationary model exhibited a significant difference. For example, the nonstationary GEV_{ns-2} model fitted to *Ps* of stations 1, 2,

https://doi.org/10.5194/hess-2019-358
Preprint. Discussion started: 14 October 2019

3, and 5 showed a significant upward or downward trend of extreme quantiles with years. Compared to the temporal variability, the attributes of stations 4 and 6 with GEV_{ns-1} model showed a weaker trend which demonstrated the time variability of scale parameter of the GEV distribution. Finally, it is noteworthy that nonstationary isolines were over stationary isolines for *Ps* of stations 1 and 5 as well as *Im* of station 3 (marked in blue star in Figure 4) which meant that the stationary model would underestimate the risk for a certain return period.

Insert **Figure 3** here**.**

Insert **Figure 4** here**.**

(2) Joint return period (JRP) based on AND and KEN method:

After the nonstationary copula and GEV distribution models were selected according to several goodness-of-fit tests, the design values characterizing annual extreme rainfall events were determined through Kendall's (JRP_{ken}) or AND's joint return period (JRP_{and}) expressed by Equations (8)-(10). Although the copula model for station 5 was stationary, it was regarded as a nonstationary model because of the marginal nonstationary GEV_{ns-2} model for *Ps* or *Im*, which existed at other stations.

Since events with lower exceedance probabilities are of interest for hydrological practice and the joint return period of 50-year level is able to minimize the uncertainties of extrapolation. In this study we focused typically on events with a joint return period of JRP_{ken} (JRP_{and})=50 which means the exceedance probability was equal to 0.02.

https://doi.org/10.5194/hess-2019-358
Preprint. Discussion started: 14 October 2019

Figure 5 shows isolines of Kendall return period and AND-based return period at the 50-year level for both stationary and nonstationary models. Since the number of isolines of the nonstationary model were 60 (sample size) which might show certain overlapping areas in the isoline map, four isolines corresponding to the year 1960, 1980, 2000, and 2020 are presented for simplicity. For comparison, the JRP_{ken}(JRP_{and})-isolines derived from the corresponding stationary model, which was composed of stationary GEV and stationary copula model, are also shown. Observations belonging to each station are also presented. Although the plots for all the years are not shown, the variability of design quantiles over time showed the nonstationary behavior of the dependence structure.

From **Figure 5**, JRP_{ken} was larger than JRP_{and} for the dependence structure of the same extreme rainfall attributes, which was caused by Kendall's return period method of generating the same dangerous region, regardless of different realizations (Salvadori et al. 2011). Focusing on JRP_{ken} and JRP_{and} for station 1, the design values of *Ps* varied over time, while the design values of *Im* did not vary with time. From the horizontal direction, both the JRP_{ken}-isolines and JRP_{and}-isolines exhibited a left-moving trend, recommending a descending trend for *Ps*. The maximum *Ps* values for the year 1960 were measured as 341.6 mm and 371.5 mm corresponding to JRP_{ken} and JRP_{and}=50, respectively, while 246.4 mm and 264.8 mm is calculated as the minimum marginal values. The gap between them reached 100 mm. On the other hand, none of the JRP_{ken} and JRP_{and}-isolines exhibited a variation trend of *Im* values for

https://doi.org/10.5194/hess-2019-358
Preprint. Discussion started: 14 October 2019

station 1 from the vertical perspective, which can be attributed to the stationary GEV model for *Im* of station 1 (**Table 3**). Due to sudden changes in the magnitudes of marginal values, the Kendall isolines also crossed each other. In a similar way, the nonstationary behavior of the variables was detected from the variation of design values of extreme attributes at the other five stations compared to the isolines derived from the stationary model (denoted as black line). **Figure 5**). It is noteworthy that the stationary copula model for station 5 also exhibited the variation of design values derived from both JRP_{ken} and JRP_{and}. A weak variation of 22.3 mm for *Ps* and 4.9 mm for *Im* was detected because of the corresponding nonstationary GEV model (**Table 3**).

Insert **Figure 5** here**.**

(3) Univariate risk

The hydrological risk of a certain design extreme attribute quantile x_{T_0} can be computed using Equations. (6) and (7) on the basis of the initial return period T_0 and design life *n*. The best marginal distribution model for *Im* of station 1 as well as *Ps* of stations 4 and 6 were the stationary GEV model, so these three scenarios were not taken into consideration in this part. Except for the results of Ps of station 5, the risk results of extreme attributes of other five stations were very similar (**Figure 6**). Here, we considered the risk result of the attribute *Im* of station 2 for detailed illustration. Comparing the risk of stationary and nonstationary models, a definite conclusion can

https://doi.org/10.5194/hess-2019-358
Preprint. Discussion started: 14 October 2019

be addressed: risk can increase from the stationary condition to nonstationary condition. For example, when T_0= 50 and n=20, the risks for the stationary and nonstationary conditions were 33.24% and 46.8%, respectively. That is to say an unjustified assumption would lead to an overestimation of the risk under a certain return period and design life. For *Im* of station 2, the nonstationary risk was higher than the stationary risk when $n \leq 53$. On the other hand, the nonstationary risk was smaller than the stationary risk when $n \geq 53$. This conclusion can be detected from the *Ps* of station 1.

Once T_0 was decided, the risk changing rate was calculated by equation (17). Here, T_0 was set as 50 for illustration. For attribute *Im*, the risk changing rate $\Delta R_{T_0}^n$ corresponding to T_0=50 was 45.93%, 5.31%, 18.25%, 39.44% and 37.10% for stations 2, 3, 4, 5 and 6, respectively. For attribute *Ps*, $\Delta R_{T_0}^n$ was 61.26%, 22.47%, 59.51% and 20.53% for stations 1, 2, 3 and 5. Generally, *Im* of station 2 and *Ps* of station 1 should be paid more attention with the highest risk changing rate in hydrological practice.

Insert **Figures 6** here**.**

(3) Bivariate risk based on JRP_{ken} and JRP_{and}

The hydrological nonstationary risk in the bivariate case cannot be calculated until the most likely event at T_0-year level is generated. In this part, we first focused on the development of the most likely design events where the joint probability density functions had their maximum values on the 50-year level. **Figures 7(a)** and **(b)** illustrate

https://doi.org/10.5194/hess-2019-358
Preprint. Discussion started: 14 October 2019

Hydrology and Earth System Sciences Discussions
Open Access
EGU

the time dependent development of both variables *Ps* (upper panel) and *Im* (lower panel) through the JRP_{ken} and JRP_{and} methods. The attribute *Ps* for stations 1, 2, and 3 showed a positive trend, while attribute *Im* for stations 4 and 5 exhibited a negative trend through the JRP_{ken} and JRP_{and} methods. On the other hand, the trend of the design value of Im was not significant.

The hydrological nonstationary risk based on JRP_{ken} and JRP_{and} was computed using equations (15)-(16). **Figures 8(a)** and **(b)** show the nonstationary risk *R* of the most likely design combinations of *Ps* and *Im* at the T_0-year level. The risk results of extreme attributes of stations 1, 3, 4, and 6 were very similar, while the results of stations 2 and 5 exhibited a similar pattern. For stations 1, 3, 4, and 6, the risk increased with design life *n* under both stationary and nonstationary conditions, but for any T_0, the nonstationary risk was higher than stationary risk from both JRP_{ken} and JRP_{and} methods. For stations 2 and 5, the nonstationary risk was lower than stationary risk from both the JRP_{ken} and JRP_{and} methods. The corresponding changing rate to quantify the differences in hydrological risk for the bivariate case between stationary and nonstationary models was also calculated by equation (17). Whether it was calculated through the JRP_{ken} and JRP_{and} methods, the changing risk rate increased as T_0 increased, which meant that nonstationarity influenced the risk of lower exceedance probabilities more than that of higher exceedance probabilities.

Since a 50-year level with lower exceedance probabilities (0.02) is of great interest in hydrological practice and necessary to control the uncertainties of extrapolation

https://doi.org/10.5194/hess-2019-358
Preprint. Discussion started: 14 October 2019

Hydrology and Earth System Sciences
Discussions

(Bender et al., 2014), in this part, we focused on the risk changing rate under the 50 year-level for each station. For JRP_{and}, the risk changing rate $\Delta R_{T_0}^{n}$ corresponding to T_0=50 was 41.83%, 7.96%, 24.27%, 6.94%, 9.21%, and 70.63% for stations 1, 2, 3, 4, 5, and 6, respectively. For JRP_{ken}, the risk changing rate $\Delta R_{T_0}^{n}$ corresponding to T_0=50 was 59.93%, 8.44%, 44.19%, 10.69%, 11.96%, and 75.29% for stations 1, 2, 3, 4, 5, and 6, respectively. According to the above results of risk changing rate, changing risk rates based on the JRP_{ken} method were higher than those through the JRP_{and} method, which indicated that the JRP_{ken}-based risk was more sensitive to the nonstationarity of marginal and bivariate distribution models.

Insert **Figures 7(a)-(b)** here**.**

Insert **Figures 8(a)-(b)** here**.**

4.6. Further discussion

Based on the above analysis, the nonstationary risk analysis over extreme rainfall events using the time-varying GEV and copula-based distribution models were distinguished from those where the partial assumption of stationarity was employed (**Figures 4-8**). These results showed the significance of considering nonstationarity when calculating return period and hydrological risk both in univariate and bivariate cases. There were also certain differences between the results using Kendall’s joint return period method and AND’s return period method. *Im* of station 2 and *Ps* of station

1 should be concerned with the highest risk changing rate from the perspective of univariate case, while the dependence structure of station 6 should be paid more attention with the highest risk changing rate from the perspective of bivariate case.

According to the results performed by the proposed time-varying models, the following points should be emphasized:

- ✓ It is necessary to use statistical tests, such as the Ljung-Box test, univariate and multivariate Mann-Kendall test, and univariate and multivariate Pettitt test to evaluate nonstationarities of extreme rainfall attributes (*Ps* and *Im*) as well as the dependence between these two attributes. These two attributes corresponding to six stations showed no serial correlation which rationalized the implementation of traditional multivariate Mann-Kandall tests without any modification.
- ✓ Nonstationarity in the dependence structure and marginal variable was non-ignorable. The nonstationary (time-varying) GEV and copula-based model not only addressed the abrupt changes and significant trends existed in the marginal variables, but also evaluated the dependence of multivariate hydrological series, which led to the reliable estimation of hydraulic design quantiles.
- ✓ The traditional hydrological risk under nonstationary conditions in the univariate case was expanded to the bivariate case through the Kendall joint return period method and AND return period method. According to the return

https://doi.org/10.5194/hess-2019-358
Preprint. Discussion started: 14 October 2019

period analysis in the univariate case, the scale parameter of the nonstationary GEV distribution demonstrated a significant time variability for uncertainty. The joint return period and risk analysis also showed that the JRP_{ken}-based risk was more sensitive to the nonstationarity of marginal and bivariate distribution models.

Moreover, the two indexes used in this study, revealing the characteristics of extreme rainfall events, i.e., *Ps* and *Im*, representing rainfall volume and intensity, respectively were extracted from observed daily precipitation datasets. Risk analysis based on these two attributes helped understand extreme rainfall patterns, especially storm events lasting several days, which would be devastating to urban infrastructure and farmlands. In addition, the duration which is another meaningful extreme rainfall attribute should also be incorporated into multivariate risk analysis.

5. Conclusions

In this paper, a nonstationary risk analysis through the time-varying Generalized Extreme Value (GEV) and copula-based distribution model is performed over the extreme rainfall events in Haihe River Basin. The time-dependent copula and GEV models are applied to these two attributes (*Ps* and *Im*) extracted from daily rainfall data of six stations in Haihe River basin, China. Nonstationarity and trends in the attribute series were investigated through multivariate Mann-Kendall test and multivariate Pettist test. The best nonstationary GEV model was selected for the attribute of each

https://doi.org/10.5194/hess-2019-358
Preprint. Discussion started: 14 October 2019

station through the minimum *DIC* criterion combined with the Bayes factor (*BF*) test, while the best-fitted time-varying copula was selected through the minimum Corrected Akaike Information Criterion (AICc). Based on frequency analysis by the Kendall joint return period method and the AND return period method, the design values of the two indexes were computed and shown by the JRP_{ken}-isolines and JRP_{and}-isolines. The extended bivariate nonstationary DLL-based risk was calculated through the estimated most likely event (combinations of *Ps* and *Im*) to quantify the risk of each station under nonstationary conditions. Analysis of extreme rainfall occurrence risk based on the observed index series demonstrated that station 6 should be paid more attention with the highest risk changing rate. The following conclusions can be drawn from this study:

1. A 100-year Ps quantile under stationary conditions (355 mm) can correspond to a 35-year Ps under nonstationary conditions. In other words, an exceedance probability of 0.01 can increase to 0.028 and 0.017. On the other hand, the return period associated with a given quantile can decrease for Im of some stations but can increase for other stations.
2. The stationary model would underestimate the risk for a certain return period.
3. From the marginal return period to the joint return period, there can be a significant upward or downward trend in extreme quantiles in the univariate case which can change into a weak trend in the joint return period.
4. Nonstationarity influences the risk of lower exceedance probabilities more than that of higher exceedance probabilities.

5. Changing risk rates based on the JRP_{ken} are higher than those based on the JRP_{and} method, which indicated that the JRP_{ken}-based risk is more sensitive to the nonstationarity of marginal and bivariate distribution models.

This study emphasizes the significance of incorporating nonstationarity into multivariate risk analysis through the investigation of univariate and multivariate trend and change points in the attribute series. The Kendall return period is justified as more practical method for hydraulic design than the AND return period method according to the calculation of the design quantiles for the extreme rainfall. The extended bivariate nonstationary DLL-based risk method was applied to both stationary and nonstationary conditions.

Acknowledgments

This study was supported by the National Key Research and Development Program of China (2017YFC1502704，2016YFC0401501), and the National Natural Science Fund of China (41571017, 51679118 and 91647203), and Jiangsu Province"333 Project" (BRA2018060).

https://doi.org/10.5194/hess-2019-358
Preprint. Discussion started: 14 October 2019

References

Agilan, V., and Umamahesh, N.V.: Covariate and parameter uncertainty in non-stationary rainfall IDF curve, Int. J. Climatol., 38, 365-383, https://doi.org/10.1002/joc.5181, 2018.

Ali, H., and Mishra, V.: Increase in subdaily precipitation extremes in India under 1.5 and 2.0 ℃ warming worlds. Geophys, Res. Lett., 45, 6972–6982, https://doi.org/10.1029/2018GL078689, 2018.

Aissia, M.A.B., Chebana, F., Ouarda, T.B.M.J., Roy, L., Bruneau, P., and Barbet, M.: Dependence evolution of hydrological characteristics, applied to floods in a climatechange context in Quebec, J. Hydrol., 519, 148–163, https://doi.org/10.1016/j.jhydrol.2014.06.042, 2014

Bender, J., Wahl, T., and Jensen, J.: Multivariate design in the presence of non-stationarity, J. Hydrol., 514, 123–130, https://doi.org/10.1016/j.jhydrol.2014.04.017, 2014.

Call, B.C., Belmont, P. Schmidt, J.C., and Wilcock, P.R.: Changes in floodplain inundation under nonstationary hydrology for an adjustable, alluvial river channel, Water Resour. Res., 53(5), 3811-3834, https://doi.org/10.1002/2016WR020277, 2017.

Chebana, F., Ouarda, T.B., and Duong, T.C.: Testing for multivariate trends in hydrologic frequency analysis, J. Hydrol., 486, 519–530, https://doi.org/10.1016/j.jhydrol.2013.01.007, 2013.

Chen, H., and Sun, J.: Contribution of human influence to increased daily precipitation

https://doi.org/10.5194/hess-2019-358
Preprint. Discussion started: 14 October 2019

extremes over china, Geophys. Res. Lett., 44(5), 2436-2444, https://doi.org/10.1002/2016GL072439, 2017.

Cheng, L., and AghaKouchak, A.: Nonstationary precipitation intensity-duration-frequency curves for infrastructure design in a changing climate, Sci. Rep., 4, 7093, https://doi.org/10.1038/srep07093, 2014.

Cheng, L., AghaKouchak, A., Gilleland, E., and Katz, R.W.: Nonstationary extreme value analysis in a changing climate, Clim. Change, 127, 353–369, https://doi.org/10.1007/s10584-014-1254-5, 2014.

Condon, L.E., Gangopadhyay, S., and Pruitt, T.: Climate change and non-stationary flood risk for the upper Truckee River basin, Hydrol. Earth Syst. Sci., 19, 159–175, https://doi.org/10.5194/hess-19-159-2015, 2015.

De Michele, C., Salvadori, G., Vezzoli, R., and Pecora, S.: Multivariate assessment of droughts: frequency analysis and dynamic return period, Water Resour. Res., 49(10), 6985–6994, https://doi.org/10.1002/wrcr.20551, 2013.

Donat, M.G., Lowry, A.L., Alexander, L.V., O'Gorman, P.A., and Maher, N.: More extreme precipitation in the world's dry and wet regions, Nat. Clim. Change, 6, 508–513, https://doi.org/10.1038/nclimate2941, 2016.

Du, T., Xiong, L.H., Xu, C.Y., Gippel C.J., Guo, S.L., and Liu, P.: Return period and risk analysis of nonstationary low-flow series under climate change, J. Hydrol., 527, 234-250, https://doi.org/10.1016/j.jhydrol.2015.04.041, 2015.

Ganguli, P., and Coulibaly, P.: Does nonstationarity in rainfall requires nonstationary intensity-duration-frequency curves? Hydrol. Earth Syst. Sci., 21(12), 1-31,

https://doi.org/10.5194/hess-2019-358
Preprint. Discussion started: 14 October 2019

Hydrology and Earth System Sciences
Open Access
Discussions

https://doi.org/10.5194/hess-21-6461-2017, 2017.

Ghanbari, M., M. Arabi, J. Obeysekera, and Sweet, W.: A coherent statistical model for coastal flood frequency analysis under nonstationary sea level conditions, Earth's Future, 7, 162-177, https://doi.org/10.1029/2018EF001089, 2017.

Gräler, B., van den Berg, M.J., Vandenberghe, S., Petroselli, A., Grimaldi, S., De Baets, B., and Verhoest, N.E.C.: Multivariate return periods in hydrology: a critical and practical review focusing on synthetic design hydrograph estimation, Hydrol. Earth Syst. Sci., 17, 1281-1296, https://doi.org/10.5194/hess-17-1281-2013, 2013.

Grimaldi, S., and Serinaldi, F.: Asymmetric copula in multivariate flood frequency analysis, Adv. Water Resour., 29(8), 1155–1167, https://doi.org/10.1029/2018EF001089, 2006.

Gu, X., Zhang, Q., Singh, V.P., Chen, X., and Liu, L.: Nonstationarity in the occurrence rate of floods in the Tarim River Basin, China, and related impacts of climate indices, Global Planet. Change, 142, 1-13, https://doi.org/10.1016/j.gloplacha.2016.04.004, 2016.

Jakob, D., AghaKouchak, A. Easterling, D., Hsu, K., Schubert, S., and Sorooshian, S. (Eds.): Nonstationarity in extremes and engineering design, Springer, New York, 2013.

Jiang, C., Xiong, L., Xu, C.Y., and Guo, S.: Bivariate frequency analysis of nonstationary low-flow series based on the time-varying copula, Hydrol. Process., 29(6), 1521-1534, https://doi.org/10.1002/hyp.10288, 2015.

Kao, S., and Govindaraju, R.S.: Trivariate statistical analysis of extreme rainfall events via the Plackett family of copulas, Water Resour. Res., 44 (2), 333–341, https://doi.org/10.1029/2007WR006261, 2008.

Lima, C.H.R., Kwon, H.H., and Kim, J.Y.: A bayesian beta distribution model for estimating rainfall idf curves in a changing climate, J. Hydrol., 540, 744-756, https://doi.org/10.1016/j.jhydrol.2016.06.062, 2016.

Liu, J., Zhang, Q., Singh, V.P., Gu, X., and Shi, P.: Nonstationarity and clustering of flood characteristics and relations with the climate indices in the Poyang Lake Basin, China, Hydrolog. Sci. J., 62 (11), 1809–1824, https://doi.org/10.1080/02626667.2017.1349909, 2017.

Madsen, H., Gregersen, I.B., Rosbjerg D., and Arnbjerg-Nielsen, K.: Regional frequency analysis of short duration rainfall extremes using gridded daily rainfall data as co-variate, Water Sci. Technol., 75(8),1971-1981, https://doi.org/10.2166/wst.2017.089, 2017.

Martins, E.S., and Stedinger, J.R.: Generalized maximum likelihood generalized extreme-value quantile estimators for hydrologic data, Water Resour. Res., 36, 737–744, https://doi.org/10.1029/1999wr900330, 2000.

Milly, P.C.D., Betancourt J., Falkenmark, M., Hirsch, R.M., Kundzewicz, Z.W., and Lettenmaier, D.P.: On critiques of “stationarity is dead: whither water management?”, Water Resour. Res., 51(9), 7785-7789, https://doi.org/10.1002/2015wr017408, 2015.

Mishra, A. K., and Singh, V. P.: Analysis of drought severity-area-frequency curves using a general circulation model and scenario uncertainty, J. Geophys. Res. Atmos., 114(D6), https://doi.org/10.1029/2008JD010986, 2009.

Nelsen, R.B.: An introduction to copulas, Springer, New York, 2007.

Patton, A.J.: Modelling asymmetric exchange rate dependence, Int. Econ. Rev., 47(2), 527–556, https://doi.org/10.2307/3663514, 2006.

Porporato, A., and Ridolfi, L.: Influence of weak trends on exceedance probability, Stoch. Hydrol. Hydraul., 12, 1–14, https://doi.org/10.1007/s004770050006,1998.

Rauf, U.F.A., and Zeephongsekul, P.: Copula based analysis of rainfall severity and duration: a case study, Theor. Appl. Climatol., 115(1–2), 153–166, https://doi.org/10.1007/s00704-013-0877-1, 2014.

Rizzo, M.L., and Székely, G.J: Disco analysis: a nonparametric extension of analysis of variance, Ann. Appl. Stat., 4(2), 1034-1055, https://doi.org/10.1214/09-AOAS245, 2010.

Renard, B., and Lang, M.: Use of a gaussian copula for multivariate extreme value analysis: some case studies in hydrology, Adv. Water Resour., 30(4), 897-912, https://doi.org/10.1016/j.advwatres.2006.08.001, 2007.

Rootzén, H., and Katz, R.W.: Design Life Level: Quantifying risk in a changing climate, Water Resour. Res., 49(9), 5964-5972, https://doi.org/10.1002/wrcr.20425,2013.

Sarhadi, A., and Soulis, E.D.: Time-varying extreme rainfall intensity-duration-frequency curves in a changing climate, Geophys, Res. Lett., 44(5), 2454-2463, https://doi.org/10.1002/2016GL072201, 2017.

Salvadori, G., and De Michele, C.: Frequency analysis via copulas: theoretical aspects and applications to hydrological events, Water Resour. Res., 40(12), 229–244, https://doi.org/10.1029/2004wr003133, 2004.

Salvadori, G., and De Michele, C.: Multivariate multiparameter extreme value models and return periods: A copula approach, Water Resour. Res., 46, W10501, https://doi.org/10.1029/2009WR009040, 2010.

Salvadori, G., De Michele, C., and Durante, F.: On the return period and design in a multivariate framework, Hydrol. Earth Syst. Sci., 15(11), 3293–3305, https://doi.org/10.5194/hess-15-3293-2011, 2011.

Salvadori, G., Durante, F., and De Michele, C.: Multivariate return period calculation via survival functions, Water Resour. Res., 49(4), 2308-2311, https://doi.org/10.1002/wrcr.20204, 2013.

Salas, J.D., and Obeysekera, J.: Revisiting the concepts of return period and risk for non-stationary hydrologic extreme events, J. Hydrol. Eng., 19, 554–568, https://doi.org/110.1061/(ASCE)HE.1943-5584.0000820, 2014.

Serinaldi, F., Bonaccorso, B., Cancelliere, A., and Grimaldi, S.: Probabilistic characterization of drought properties through copulas, Phys. .Chem. Earth, 34(10–12),596–605, https://doi.org/10.1016/j.pce.2008.09.004, 2009.

Serinaldi, F., and Kilsby, C.G.: Stationarity is undead: uncertainty dominates the distribution of extremes, Adv. Water Resour., 77, 17-36, https://doi.org/10.1016/j.advwatres.2014.12.013, 2015.

Serinaldi, F., and Kilsby, C.G.: The importance of prewhitening in change point analysis under persistence, Stoch. Env. Res. Risk A., 30(2), 763-777, https://doi.org/10.1007/s00477-015-1041-5, 2016.

https://doi.org/10.5194/hess-2019-358
Preprint. Discussion started: 14 October 2019

Shiau, J.T.: Fitting drought duration and severity with two-dimensional copulas, Water Resour. Manag., 20(5), 795–815, https://doi.org/10.1007/s11269-005-9008-9, 2006.

Song, S., and Singh,V.P.: Meta-elliptical copulas for drought frequency analysis of periodic hydrologic data, Stoch. Env. Res. Risk A., 24(3), 425–444, https://doi.org/10.1007/s00477-009-0331-1, 2010.

Vandenberghe, S., Verhoest, N.E.C., and Baets, B.D.: Fitting bivariate copulas to the dependence structure between storm characteristics: a detailed analysis based on 105 year 10 min rainfall, Water Resour. Res.,46 (1), 489–496, https://doi.org/10.1029/2009WR007857,2010.

Wong, G., Lambert, M.F., Leonard, M., and Metcalfe, A.V.: Drought analysis using trivariate copulas conditional on climatic states, J. Hydrol. Eng., 15(2), 129–141, https://doi.org/10.1061/(ASCE)HE.1943-5584.0000169, 2010.

Zhang, Q. , Gu, X. , Singh, V. P. , and Chen, X.: Evaluation of ecological instream flow using multiple ecological indicators with consideration of hydrological alterations, J. Hydrol., 529, 711-722, https://doi.org/10.1016/j.jhydrol.2015.08.066, 2015.

Yan, L., Xiong, L., Guo, S., Xu, C.-Y., Xia, J., and Du, T.: Comparison of four nonstationary hydrologic design methods for changing environment, J. Hydrol., 551, 132–150, https://doi.org/10.1016/j.jhydrol.2017.06.001, 2017.

Yilmaz, A. G., Imteaz, M. A., and Perera, B.J.C.: Investigation of non-stationarity of extreme rainfalls and spatial variability of rainfall intensity-frequency-duration relationships: a case study of Victoria, Australia, Int. J. Climatol., 37, 430–442, https://doi.org/10.1002/joc.4716, 2017.

Yilmaz, A.G., and Perera, B.J.C.: Extreme rainfall nonstationarity investigation and intensity-frequency-duration relationship, J. Hydrol. Eng., 19(6), 1160–1172, https://doi.org/10.1061/(ASCE)HE.1943-5584.0000878,2014.

Zhang, L., and Singh, V.P.: Bivariate flood frequency analysis using the copula method, J. Hydrol. Eng., 11(2), 150–164, https://doi.org/10.1061/(ASCE)1084-0699(2006)11:2(150), 2006.

Zhang, L., and Singh, V.P.: Bivariate rainfall frequency distributions using Archimedean copulas, J. Hydrol., 332(1), 93–109, https://doi.org/10.1016/j.jhydrol.2006.06.033, 2007.

https://doi.org/10.5194/hess-2019-358
Preprint. Discussion started: 14 October 2019

Hydrology and Earth System Sciences
Open Access
Discussions

Lists of Tables

https://doi.org/10.5194/hess-2019-358
Preprint. Discussion started: 14 October 2019

Hydrology and Earth System Sciences
Discussions

Lists of Figures

https://doi.org/10.5194/hess-2019-358
Preprint. Discussion started: 14 October 2019

Table 1. Information on meteorological gauges of Haihe River basin

	Station ID	Station name	Location		Data range
			Longtitude	Latitude	
1	53588	Wutaishan	113°32′	39°02′	1952-2017
2	54308	Fengning	116°32′	41°12′	1957-2017
3	54401	Zhangjiakou	115°11′	40°50′	1958-2017
4	54511	Beijing	116°19′	39°57′	1958-2017
5	54527	Tianjin	117°10′	39°06′	1958-2017
6	54705	Nangon	115°23′	37°22′	1956-2017

https://doi.org/10.5194/hess-2019-358
Preprint. Discussion started: 14 October 2019

Hydrology and Earth System Sciences
Discussions

Table 2. Detection of trends and change points in extreme rainfall attributes collected from six stations

Station No.	Attribute	L-jung-Box Test	Univariate MK		Univariate Pettitt Test	Multivariate MK		Multivariate Pettitt Test
		p.value	p.value	Z statistics	p.value	p.value	Z tatistics	p.value
1	Ps	0.927	0.063	-1.856*	0.048	0.450	-0.755	0.089
	Im	0.798	0.674	0.421	0.708			
2	Ps	0.307	0.105	-1.652*	0.089	0.098	-1.645*	0.095
	Im	0.462	0.132	-1.649*	0.091			
3	Ps	0.986	0.345	-0.944	0.131	0.099*	-1.641	0.078
	Im	0.575	0.051	-1.963**	0.012			
4	Ps	0.981	0.072	-1.799*	0.098	0.055	-1.922*	0.039
	Im	0.971	0.054	-1.926*	0.089			
5	Ps	0.051	0.524	-0.638	0.801	0.606	0.516	0.589
	Im	0.747	0.214	-1.244	0.678			
6	Ps	0.815	0.226	-1.212	0.454	0.115	-1.575	0.359
	Im	0.923	0.067	-1.831*	0.024			

**and * represent statistically significant at 5% and 10% significance levels; The standardized Mann-Kendall test statistic (Z statistics) in univariate and multivariate cases indicates positive (negative) with an increasing (decreasing) trend, and statistically significant at 5% and 10% significance levels when |Z|>1.96 and |Z|>1.64 respectively; Change point tests in univariate and multivariate cases are performed at 10% significance level.

https://doi.org/10.5194/hess-2019-358
Preprint. Discussion started: 14 October 2019

Hydrology and Earth System Sciences Discussions

Table 3(a) Performance of stationary and nonstationary GEV models fitted to for the marginal distribution corresponding to each attribute (stations 1-3)

Station	Attribute	Model	μ	σ	κ	*DIC*	*BF*
1	*Ps*	GEV_s	144.37	45.32	0.058	1944.47	-
		GEV_{ns}-1	147.82+0.0014t	46.67	0.033	1943.03	0.9999
		GEV_{ns}-2	**151.85-0.00042t**	**exp(3.92-0.000038t)**	**0.019**	**1942.08**	**0.9991**
	Im	**GEV_s**	**50.64**	**18.13**	**0.012**	**1593.71**	**-**
		GEV_{ns}-1	46.69+0.0013t	17.81	0.035	1597.58	1.0011
		GEV_{ns}-2	51.7-0.00062t	exp(2.96-0.000037t)	0.019	1596.53	1.004
2	*Ps*	GEV_s	106.25	28.84	-0.12	1740.92	-
		GEV_{ns}-1	104.08-0.00018t	28.83	-0.12	1742.66	0.998
		GEV_{ns}-2	**99.92+0.0028t**	**exp(3.25+0.000057t)**	**-0.13**	**1742.29**	**0.996**
	Im	GEV_s	40.71	14.01	-0.053	1497.533	-
		GEV_{ns}-1	**42.02+0.00026t**	**14.30**	**-0.099**	**1493.47**	**0.997**
		GEV_{ns}-2	42.90-0.00031t	exp(2.39+0.00012t)	-0.082	1492.82	0.996
3	*Ps*	GEV_s	86.92	26.92	-0.077	1724.35	-
		GEV_{ns}-1	88.48+0.000096t	27.16	-0.085	1724.306	1.0002
		GEV_{ns}-2	**85.78+0.0014t**	**exp(3.57-0.00014t)**	**-0.091**	**1723.76**	**0.999**
	Im	GEV_s	34.31	11.00	0.13	1455.2	-
		GEV_{ns}-1	**37.51-0.00067t**	**11.38**	**0.10**	**1448.41**	**0.995**
		GEV_{ns}-2	41.76-0.0030t	exp(2.37+0.000019t)	0.11	1449.82	0.996

Table 3(b) Performance of stationary and nonstationary GEV models fitted for marginal distribution corresponding to each attribute (Station 2-6)

Station	Attribute	Model	μ	σ	κ	*DIC*	*BF*

https://doi.org/10.5194/hess-2019-358
Preprint. Discussion started: 14 October 2019

Hydrology and Earth System Sciences
Open Access
Discussions

4	*Ps*	GEV_s	**141.69**	**55.87**	**0.19**	**2034.265**	-
		GEV_{ns}-1	144.73-0.0016t	55.99	0.19	2036.30	1.0014
		GEV_{ns}-2	139.80-0.00014t	exp(3.88+0.000060t)	0.21	2037.05	1.0019
	Im	GEV_s	56.36	22.29	0.34	1751.59	-
		GEV_{ns}-1	**65.73-0.0035t**	**23.17**	**0.31**	**1749.31**	**0.9995**
		GEV_{ns}-2	60.33-0.00055t	exp(3.10+0.000026t)	0.31	1749.48	0.9998
5	*Ps*	GEV_s	160.34	56.07	-0.21	1963.47	
		GEV_{ns}-1	148.22+0.0016t	54.74	-0.18	1962.35	1.0002
		GEV_{ns}-2	**150.25+0.0011t**	**exp(4.07-0.000038t)**	**-0.19**	**1962.12**	**0.9999**
	Im	GEV_s	67.46	26.37	0.072	1752.36	
		GEV_{ns}-1	**77.72-0.0041t**	**26.88**	**0.047**	**1747.30**	**0.9976**
		GEV_{ns}-2	70.19-0.00072t	exp(3.66-0.00019t)	0.067	1749.53	0.9979
6	*Ps*	GEV_s	**137.56**	**57.44**	**-0.24**	**1965.79**	**-**
		GEV_{ns}-1	133.69+0.00084t	58.31	-0.25	1968.09	1.0017
		GEV_{ns}-2	138.26-0.00087t	exp(4.25-0.0001t)	-0.25	1967.70	1.0015
	Im	GEV_s	63.02	29.43	0.033	1767.72	-
		GEV_{ns}-1	69.26-0.0053t	27.93	0.059	1767.24	1.0001
		GEV_{ns}-2	**57.05+0.00083t**	**exp(3.45-0.000071t)**	**0.072**	**1766.92**	**0.9999**

https://doi.org/10.5194/hess-2019-358
Preprint. Discussion started: 14 October 2019

Table 4(a) Performance of stationary and nonstationary copula models fitted to the dependence structure of two attributes (stations 1-3)

Station	Model	Copula	*θ*	*LL*	*AICc*
1	S[a]	St[c]	0.8066	28.83	-55.59
		Clayton	1.9725	23.81	-45.55
		Gumbel	2.2677	25.08	-48.08
		Frank	8.2702	24.88	-46.55
	NS[b]	**St**	**exp(0.2998-0.0002t)**	**31.42**	**-58.71**
		Clayton	exp(-4.8096+0.0023t)	22.73	-43.39
		Gumbel	exp(-5.268+0.0256t)	23.63	-46.49
		Frank	7.677+0.00028t	21.14	-42.45
2	S	St	0.9000	51.55	-101.05
		Clayton	3.7056	42.85	-83.63
		Gumbel	3.4208	52.42	-102.77
		Frank	13.592	45.88	-89.68
	NS	**St**	**exp(0.4247-0.0003t)**	**53.46**	**-102.786**
		Clayton	exp(-3.289+0.0017t)	41.38	-80.59
		Gumbel	exp(-4.344+0.0356t)	45.57	-88.57
		Frank	10.592+0.0018t	46.07	-93.09
3	S	St	0.8491	38.25	-74.44
		Clayton	3.0403	35.57	-69.06
		Gumbel	2.6696	33.21	-64.35
		Frank	9.4212	34.89	-67.15
	NS	**St**	**exp(-1.6982+0.0008t)**	**41.49**	**-78.84**
		Clayton	*NaN*	*NaN*	*NaN*
		Gumbel	*NaN*	*NaN*	*NaN*
		Frank	11.385-0.0011t	35.18	-68.59

[a]S is stationary copula model; [b]NS represents the time-varying copula model; [c]St represents Student's t copula.

https://doi.org/10.5194/hess-2019-358
Preprint. Discussion started: 14 October 2019

Hydrology and Earth System Sciences
Open Access
Discussions

Table 4(b) Performance of stationary and nonstationary copula models fitted to the dependence structure of two attributes (stations 2-6)

Station	Model	Copula	*θ*	*LL*	*AICc*
4	S	St	0.9001	43.10	-87.13
		Clayton	2.944	36.68	-71.30
		Gumbel	3.273	46.82	-91.57
		Frank	11.462	44.68	-87.67
	NS	**St**	**exp(-1.6101+0.0008t)**	**51.79**	**-99.46**
		Clayton	exp(-3.369+0.0027t)	38.97	-75.89
		Gumbel	exp(-4.564+0.0289t)	44.68	-85.98
		Frank	12.398-0.00081t	44.68	-87.67
5	S	**St**	**0.9000**	**47.977**	**-93.886**
		Clayton	3.2678	40.62	-79.17
		Gumbel	3.1054	42.94	-83.82
		Frank	11.023	44.68	-87.67
	NS	St	exp(0.5868-0.0003t)	46.00	-91.359
		Clayton	exp(-2.987+0.0037t)	42.56	-82.69
		Gumbel	exp(-3.898+0.0252t)	41.69	-81.59
		Frank	12.589-0.00036t	42.57	-83.79
6	S	St	0.8889	43.85	-83.55
		Clayton	3.4955	44.77	-84.47
		Gumbel	2.8959	37.84	-73.61
		Frank	11.227	41.89	-81.79
	NS	**St**	**exp(0.7846-0.0005t)**	**46.02**	**-87.90**
		Clayton	exp(-3.876+0.071t)	39.59	-78.89
		Gumbel	***NaN***	***NaN***	***NaN***
		Frank	11.462	44.68	-87.67

Inf: infinite number, or out of scope of computation

https://doi.org/10.5194/hess-2019-358
Preprint. Discussion started: 14 October 2019

Hydrology and Earth System Sciences
Discussions

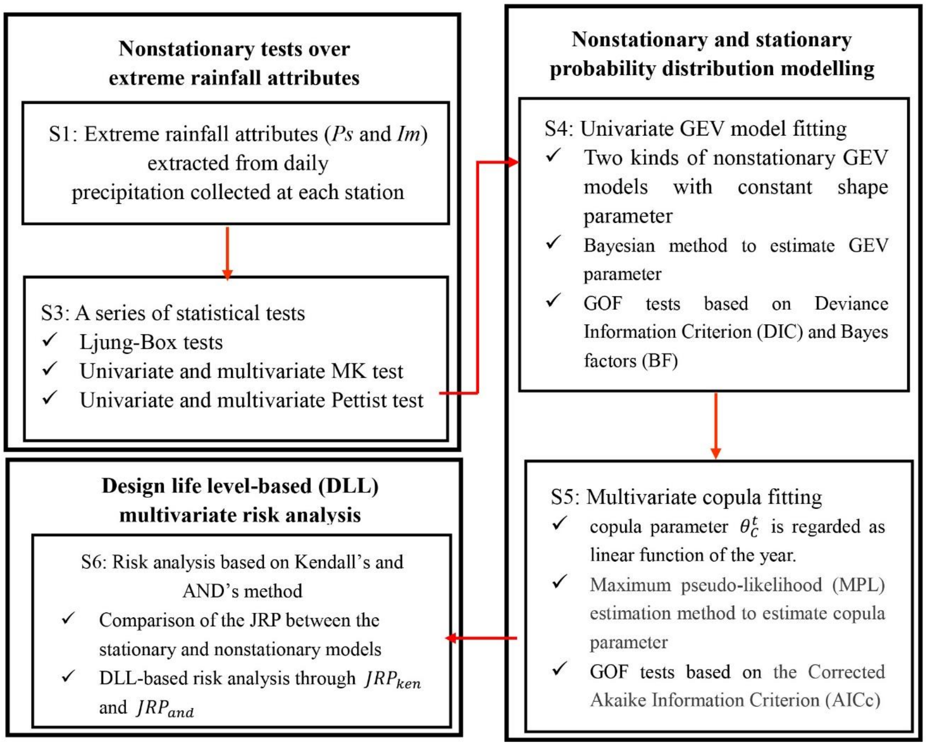

Figure 1. Flowchart of this study

https://doi.org/10.5194/hess-2019-358
Preprint. Discussion started: 14 October 2019

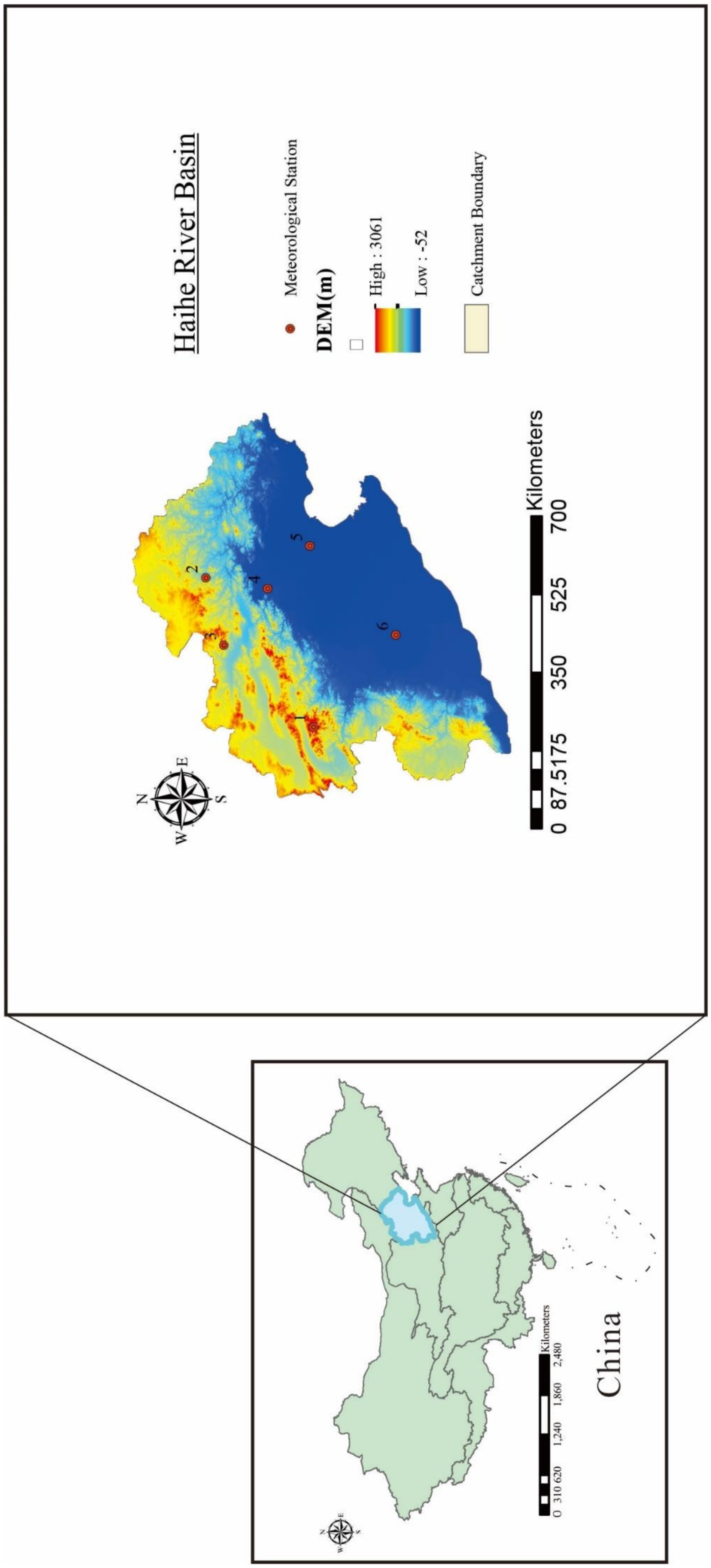

Figure 2. Selected meteorological stations in Haihe River basin

https://doi.org/10.5194/hess-2019-358
Preprint. Discussion started: 14 October 2019

Hydrology and Earth System Sciences
Discussions

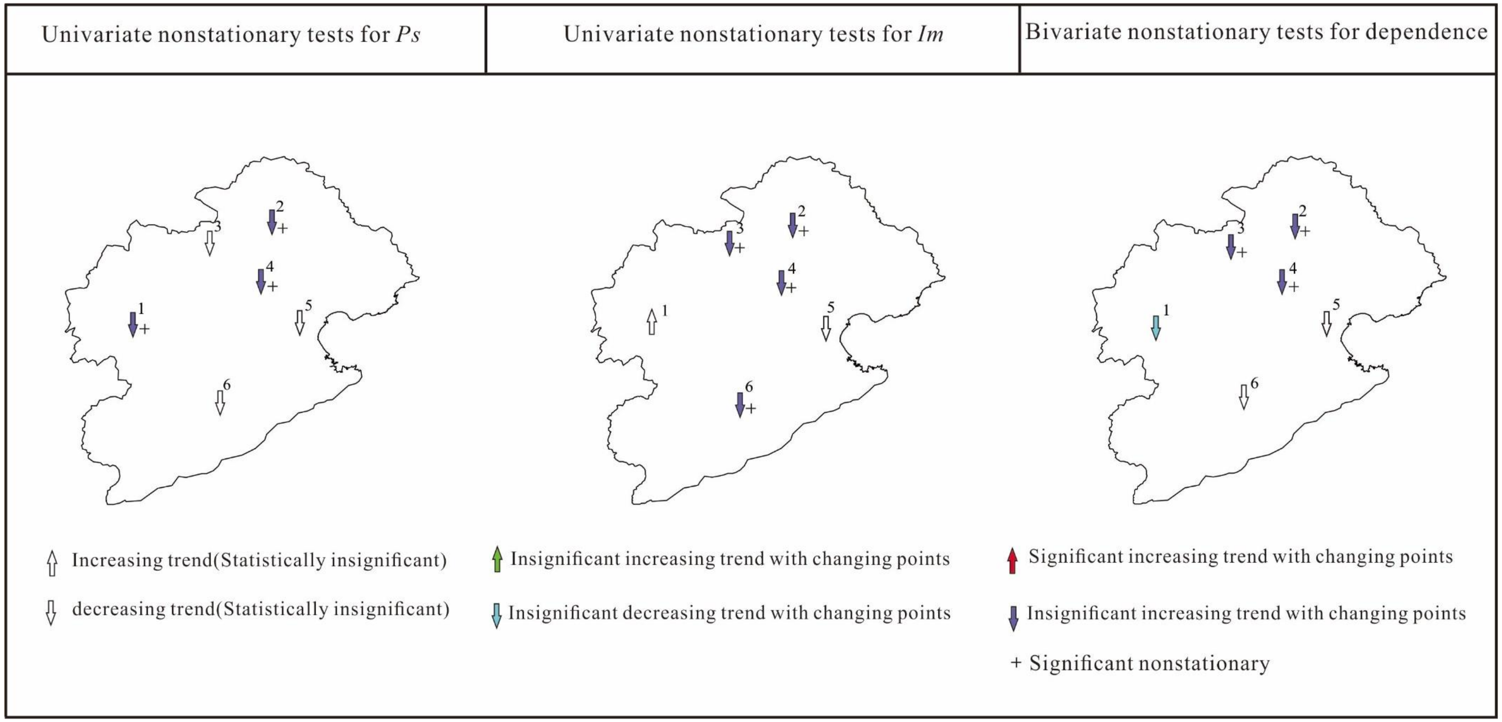

Figure 3. Spatial distribution of the trend and changing points according to univariate and multivariate Mann-Kandalld and Pettitt tests shown in Table 2; All above tests are performed at a significance level of 10%, i.e. p value< 0.10.

https://doi.org/10.5194/hess-2019-358
Preprint. Discussion started: 14 October 2019

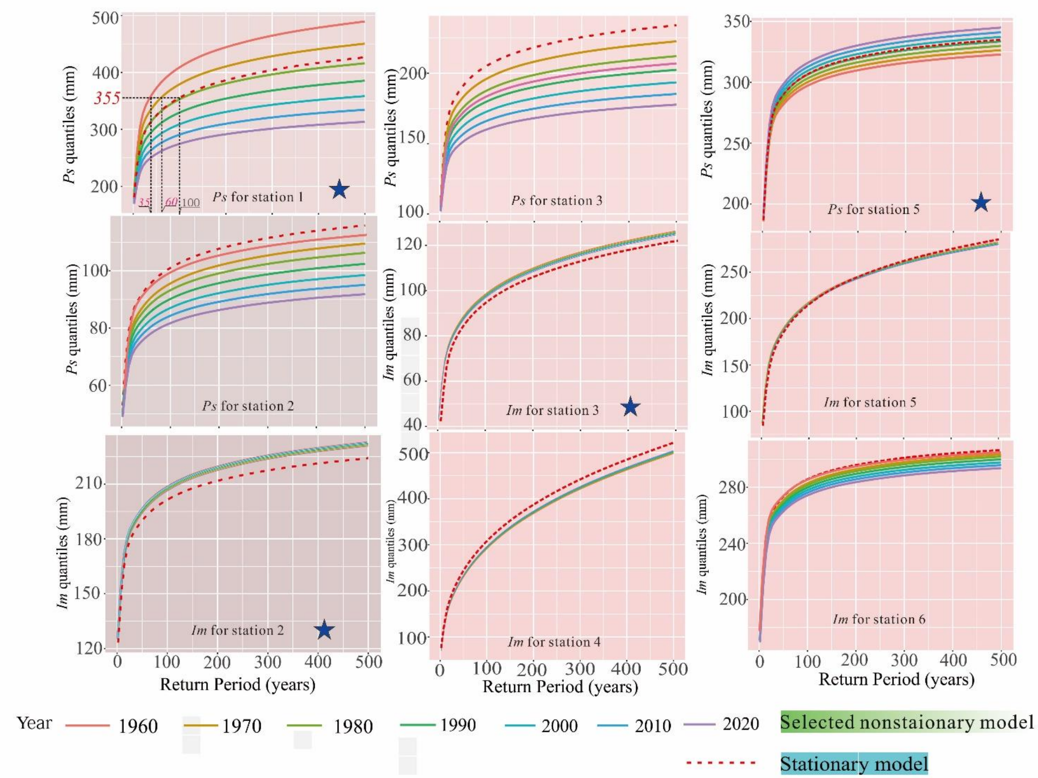

Figure 4. Estimated extreme rainfall attribute (*Ps* and *Im*) quantiles for stationary and selected nonstationary models at six stations.

https://doi.org/10.5194/hess-2019-358
Preprint. Discussion started: 14 October 2019

Hydrology and Earth System Sciences
Discussions

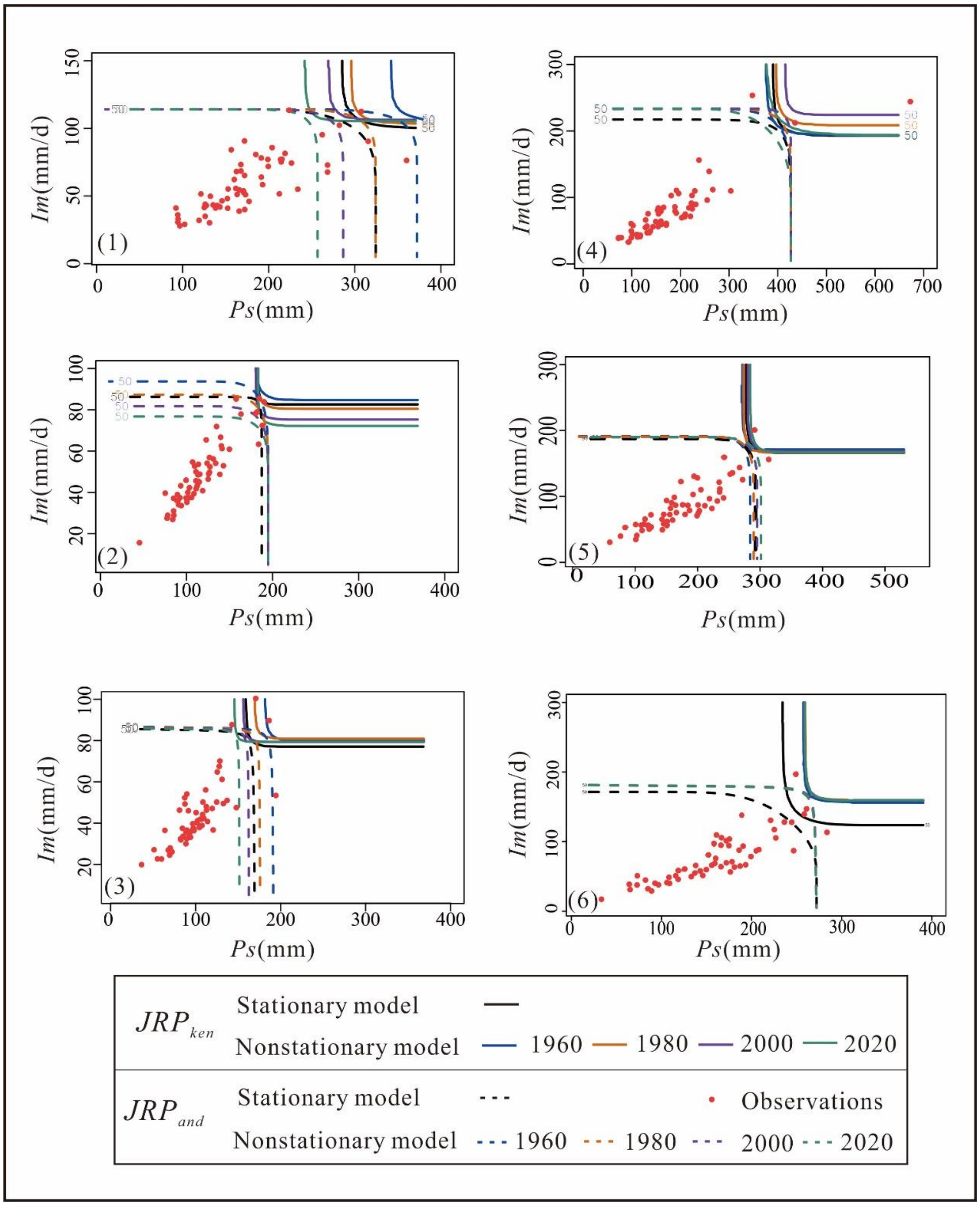

Figure 5. Isolines of Kendall return period and AND-based return period at the 50-year level for both stationary and nonstationary models. (1)-(6) represent the station number.

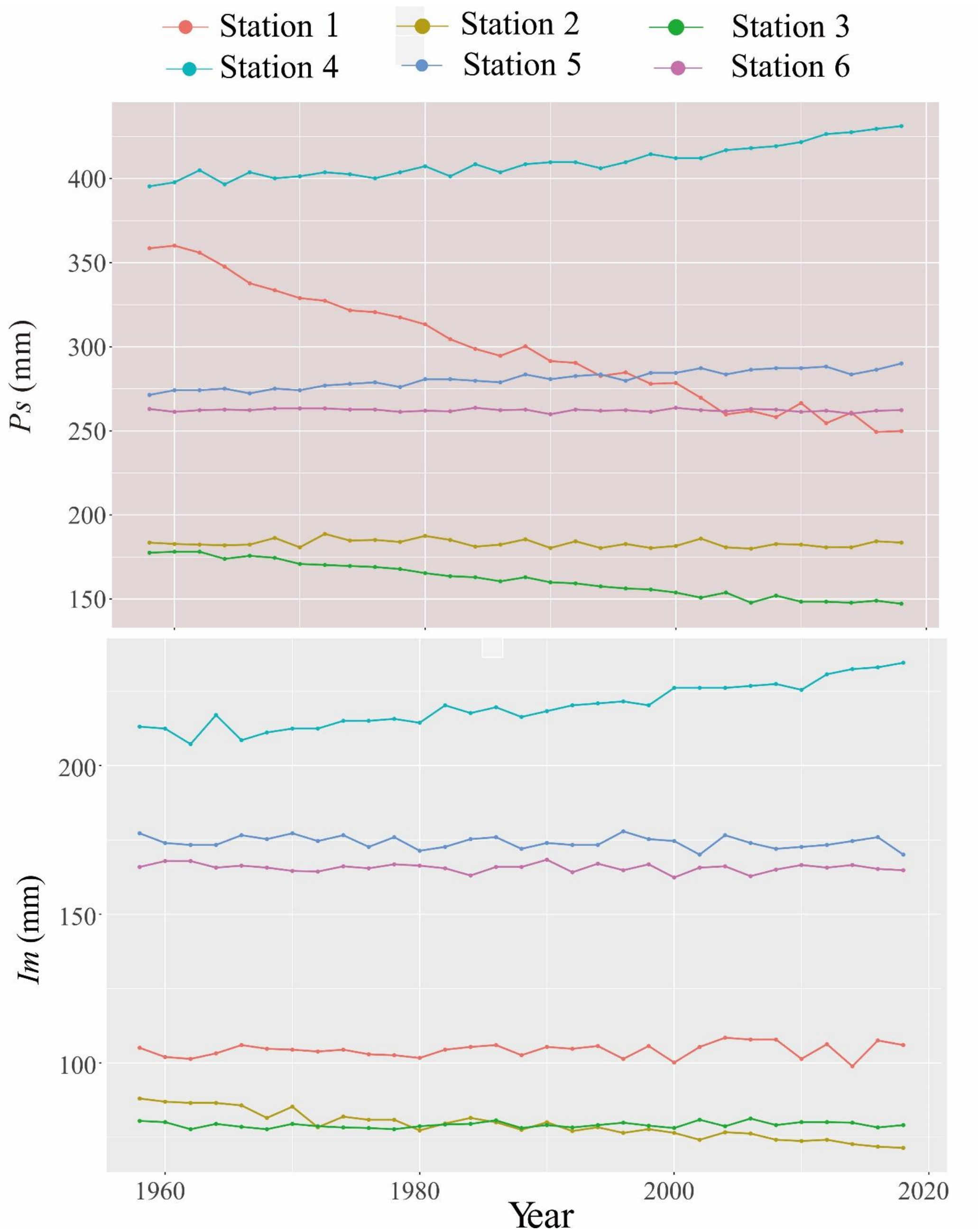

Figure 6(a). The most likely design event of Ps and Im with $JRP_{and} = 50$ for six stations

https://doi.org/10.5194/hess-2019-358
Preprint. Discussion started: 14 October 2019

Hydrology and Earth System Sciences
Discussions

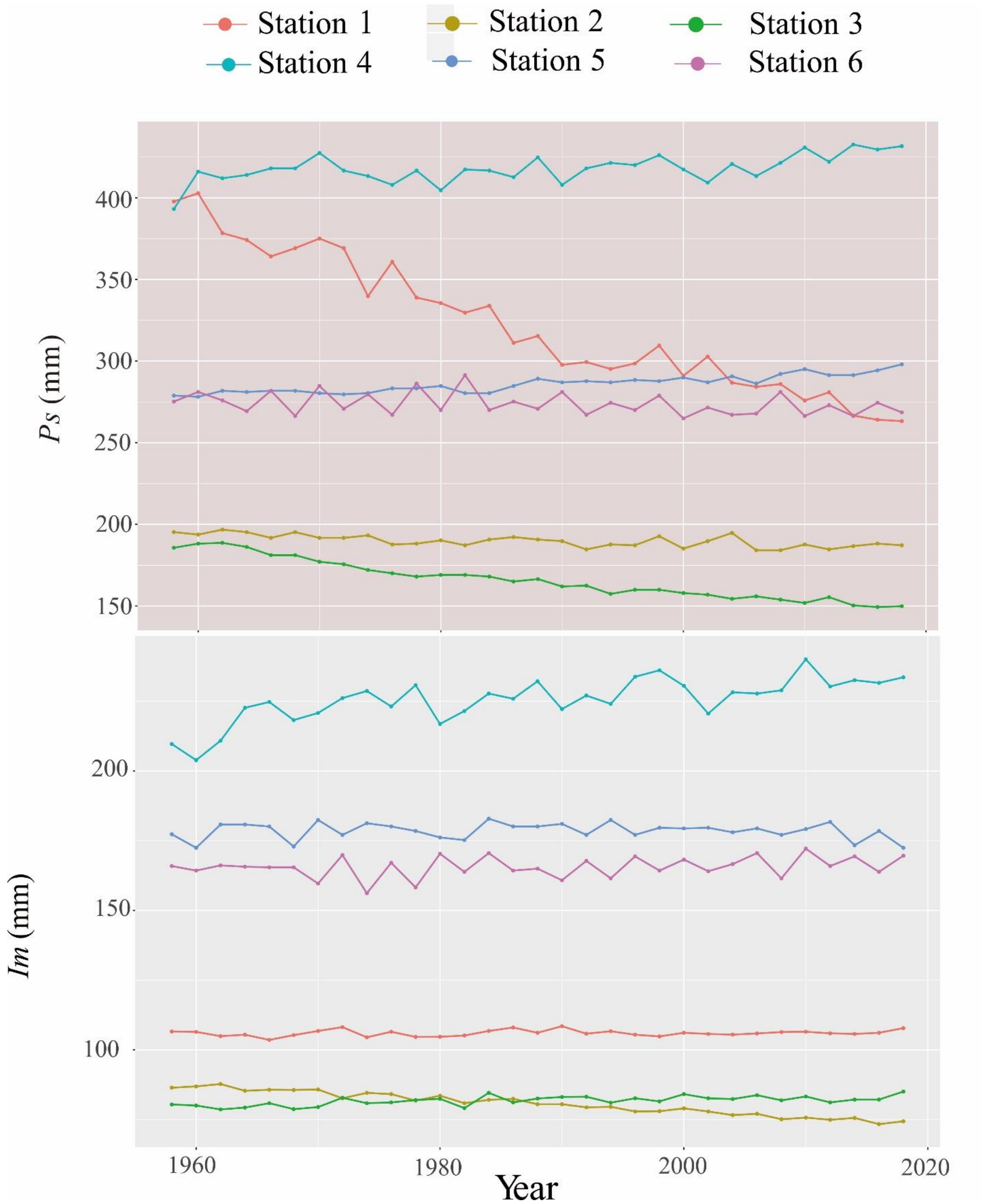

Figure 6(b). The most likely design event of Ps and Im with $JRP_{ken} = 50$ for six stations

https://doi.org/10.5194/hess-2019-358
Preprint. Discussion started: 14 October 2019

Hydrology and Earth System Sciences
Open Access
EGU
Discussions

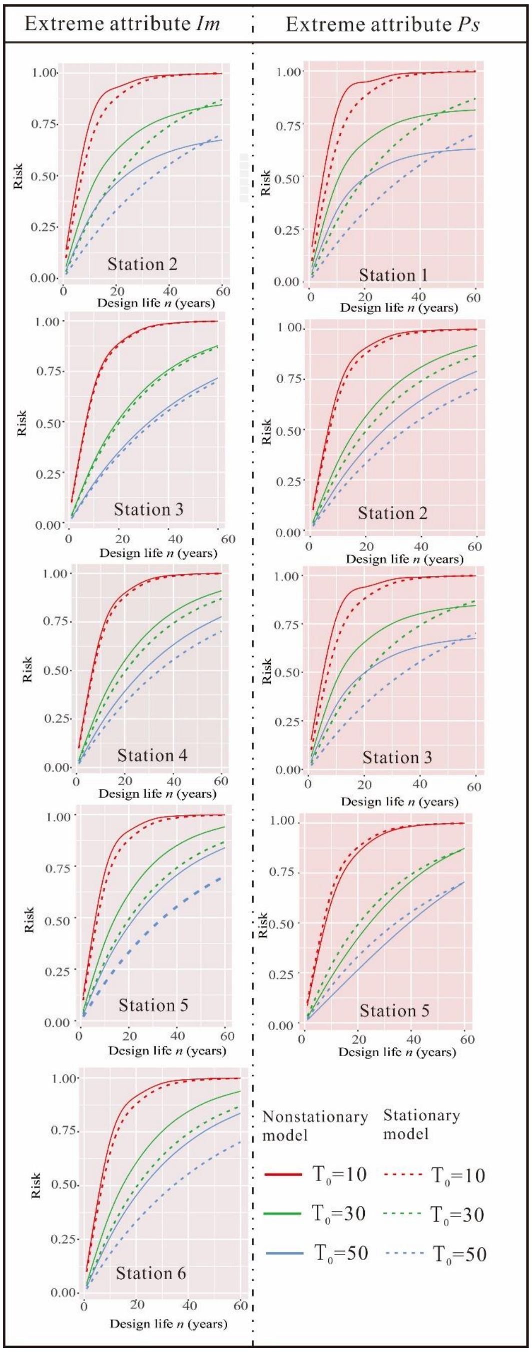

Figure 7. Nonstationary risk R of the Haihe River design extreme rainfall quantile x_{T_0} under th univariate case. The nonstationary design life level-based hydrological risk R is regarded as a function of design life n for x_{T_0} with an initial return period T_0.

https://doi.org/10.5194/hess-2019-358
Preprint. Discussion started: 14 October 2019

Hydrology and Earth System Sciences
Open Access
EGU
Discussions

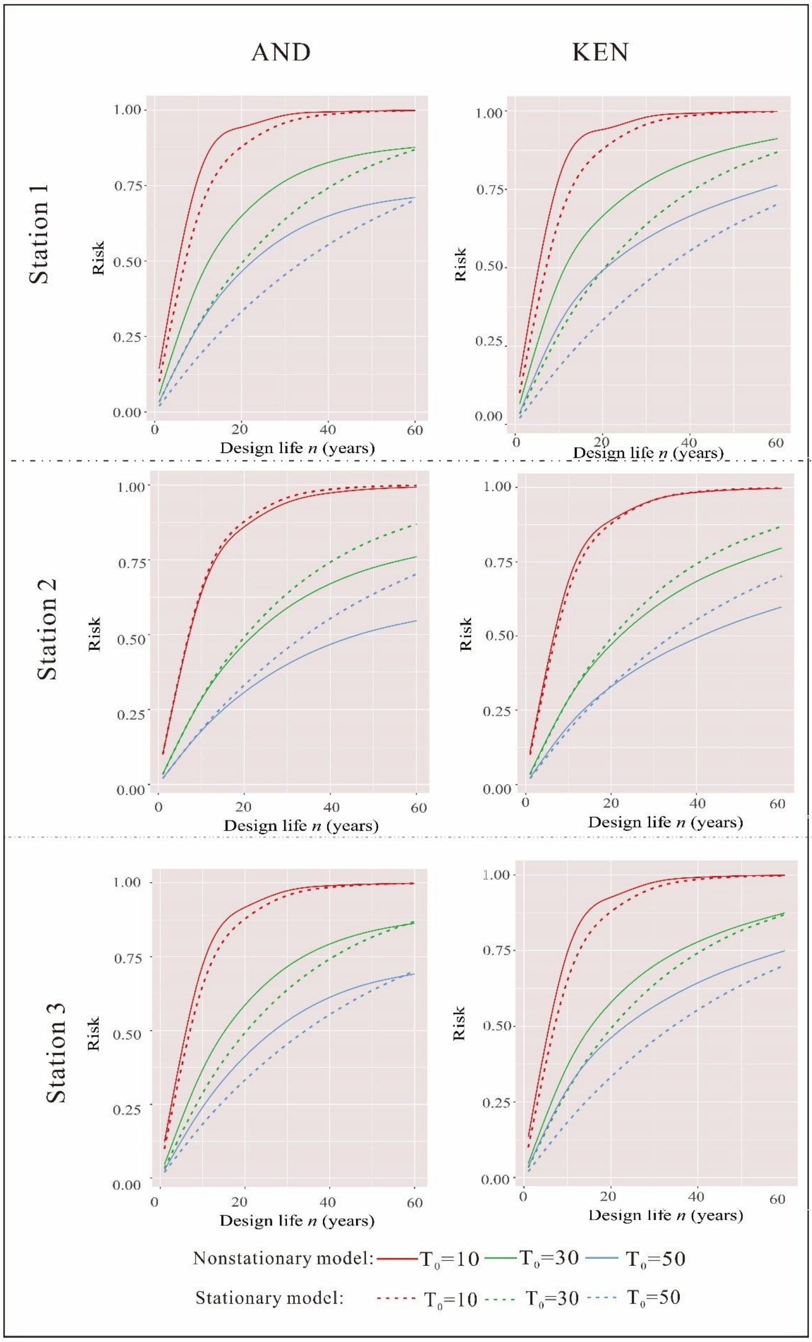

Figure 8(a). Nonstationary risk R of the most likely design combinations of *Ps* and *Im* at T_0-year level based on JRP_{s-and} and JRP_{s-ken}.

https://doi.org/10.5194/hess-2019-358
Preprint. Discussion started: 14 October 2019

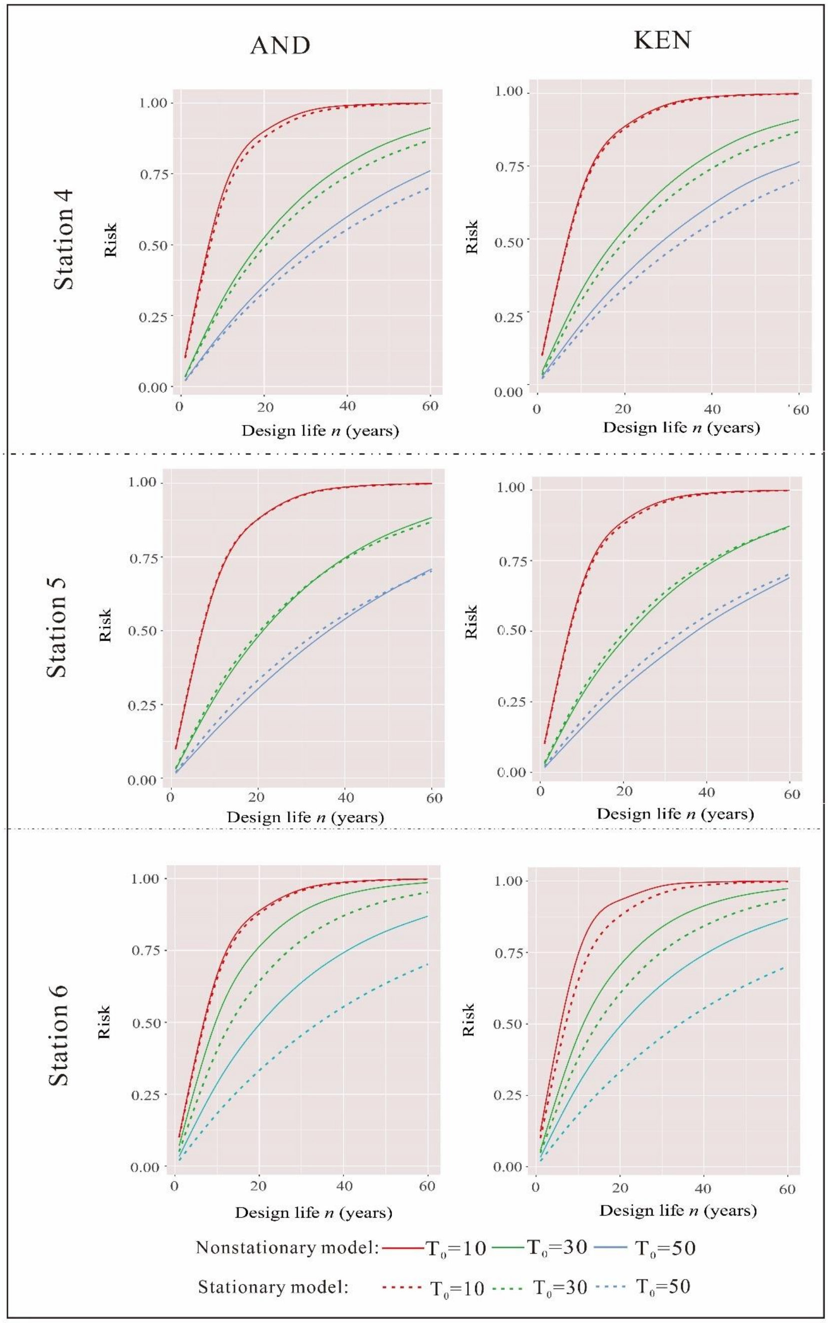

Figure 8(b). Nonstationary risk R of the most likely design combinations of *Ps* and *Im* at T_0-year level based on JRP_{s-and} and JRP_{s-ken}.